

AD-762 268

**THEORETICAL MODEL OF A SPARTON MODEL
601M HORIZONTAL VELOCITY GAGE**

Elsmer Kenneth Elkins, Jr.

**Air Force Institute of Technology
Wright-Patterson Air Force Base, Ohio**

March 1973

DISTRIBUTED BY:

NTIS

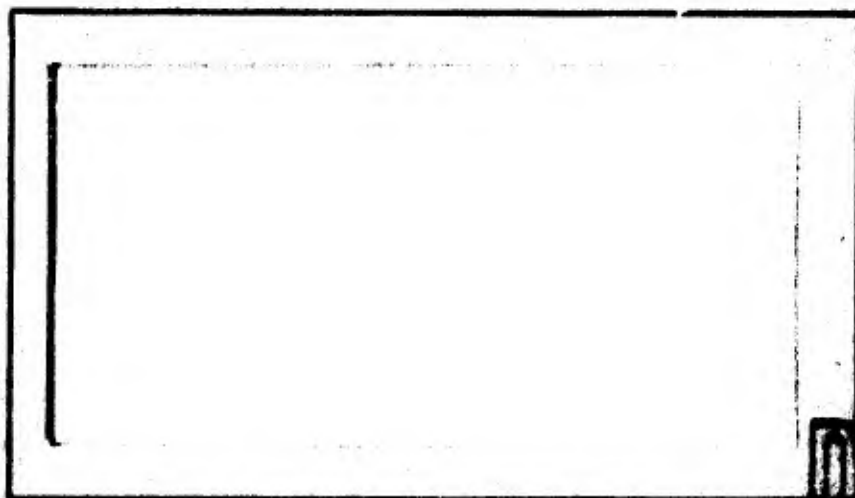
**National Technical Information Service
U. S. DEPARTMENT OF COMMERCE
5285 Port Royal Road, Springfield Va. 22151**

AD 762268

AIR FORCE INSTITUTE OF TECHNOLOGY



AIR UNIVERSITY
UNITED STATES AIR FORCE



DDC
REPRODUCED
JUN 27 1955
REGISTRY

SCHOOL OF ENGINEERING

WRIGHT-PATTERSON AIR FORCE BASE, OHIO

Reproduced by
NATIONAL TECHNICAL
INFORMATION SERVICE
U S Department of Commerce
Springfield VA 22151

91R

KEY WORDS

LINK A

LINK B

LINK C

ROLE

WT

ROLE

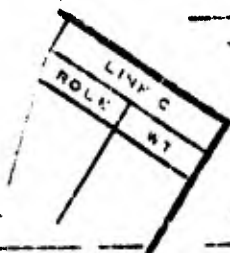
WT

ROLE

WT

Velocity of
 Bernoulli's equation
 Continuity equation
 Equation of motion
 Superficial Circulation
 Kirchhoff's Voltage Law
 System of Model
 Runge-Kutta Algorithm

16



DOCUMENT CONTROL DATA - R & D

(Type of abstract and indexing annotation must be entered when the overall report is classified)

Technology (AFIP-1)
 1473

2a. REPORT SECURITY CLASSIFICATION

Unclassified
 2b. GROUP

3. REPORT TITLE

Theoretical model of Sperton Model 601M Horizontal Velocity Gage

4. DESCRIPTIVE NOTES (Type of report and inclusive dates)

AFIP Thesis

5. AUTHOR(S) (First name, middle initial, last name)

Master Kenneth Atkins, Jr.
 Captain USAF

6. REPORT DATE

March 1973

7a. TOTAL NO. OF PAGES

29

7b. NO. OF REFS

13

8a. CONTRACT OR GRANT NO.

b. PROJECT NO.

c.

d.

8a. ORIGINATOR'S REPORT NUMBER(S)

GE/AF/73-7

8b. OTHER REPORT NO(S) (Any other numbers that may be assigned this report)

10. DISTRIBUTION STATEMENT

Approved for public release; distribution unlimited

APPROVED FOR PUBLIC RELEASE; IAFR 190-17

SPONSORING MILITARY ACTIVITY

JERRY C. HIX, Captain, USAF
 Director of Information

Air Force Weapons Lab
 Kirtland AFB, New Mexico

13. ABSTRACT

A theoretical model of a Sperton Model 601M horizontal velocity gage is developed. The mechanical and electrical systems of the velocity gage are treated as separate entities and separate models of each system are developed. Lagrange's equations are used to develop the mechanical equation of motion. Air re's circuit law is used to develop the inductance equations for the electrical model. The electrical system equations are developed by applying Kirchhoff's voltage law to an equivalent circuit for the bridge network. Then by defining state variables, the overall system equations are written. A Fortran program was developed to solve the overall system equations using a fourth order Runge-Kutta algorithm. The computer program is used to verify the overall system state model against known laboratory results. Then results are compared to indicate the linear and non-linear operating ranges of the gage. Finally, results are shown which compare the gage output to the theoretical velocity for a known dynamic input.

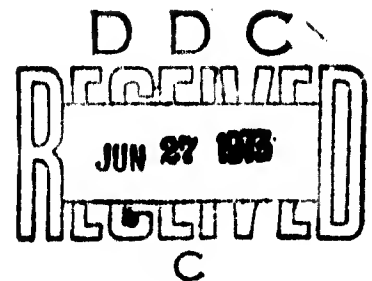
Reproduced from best available copy.

ia

THEORETICAL MODEL OF A SPARTON MODEL
601M HORIZONTAL VELOCITY GAGE

THESIS

GE/EE/73-7 Elsmer Kenneth Elkins, Jr.
 Captain USAF



Approved for public release; distribution unlimited.

THEORETICAL MODEL OF A SPARTON MODEL

601M HORIZONTAL VELOCITY GAGE

THESIS

Presented to the Faculty of the School of Engineering
of the Air Force Institute of Technology

Air University

in Partial Fulfillment of the
Requirements for the Degree of
Master of Science

by

Elsmer Kenneth Elkins, Jr., B.S.E.E.

Captain

USAF

Graduate Electrical Engineering

March 1973

Approved for public release; distribution unlimited.

ic

Preface

This thesis presents a theoretical model of a Sparton Model 601M horizontal velocity gage. This gage is manufactured by Sparton Southwest Inc. Albuquerque, New Mexico. It is used by the Air Force Weapons Laboratory, Kirtland AFB, New Mexico in conducting ground motion studies for the hardening of the Minuteman II and III complexes.

I am deeply indebted to Lt Col (Dr.) Jerry Hanson for the great amount of time he spent advising me on this thesis. I would also like to express my gratitude to Dr. Milton Franke for the advice he gave me on the fluids portion of this project. Additionally, I want to thank Prof John D'Azzo for his suggestions and Lt Col (Dr.) Giles Willis, Air Force Weapons Laboratory, for posing this most challenging problem. Finally, I would like to express my appreciation to my wife, Carol, for her understanding and help during this period of time.

Contents

| | Page |
|--|------|
| Preface | ii |
| List of Figures | iv |
| List of Tables | vi |
| List of Symbols | vii |
| Abstract | ix |
| I. Introduction | 1 |
| Background Information | 1 |
| Stanford Research Institute Velocity Gage | 2 |
| Sandia Corporation Velocity Gage | 4 |
| Sparton Model 601 Velocity Gage | 8 |
| Statement of the Problem | 8 |
| Scope of the Investigation | 9 |
| II. The Analytical Model | 10 |
| Word Description of the Velocity Gage | 10 |
| Mechanical Model | 13 |
| Kinetic Energy of the System | 15 |
| Potential Energy of the System | 20 |
| Generalized Viscous Damping Force | 21 |
| Equation of Motion | 34 |
| Electrical Model | 37 |
| Inductance Equations | 43 |
| Electrical System Equations | 47 |
| Overall System State Model | 52 |
| III. Simulation | 55 |
| Description of the Computer Program | 55 |
| Verification of the Overall System State Model | 56 |
| Operation Range of the Gage | 59 |
| Response to a Dynamic Input | 66 |
| IV. Conclusions and Recommendations | 70 |
| Bibliography | 71 |
| Appendix A: Computer Program Symbols | 72 |
| Appendix B: Computer Program Listing | 75 |

List of Figures

| Figure | Page |
|---|------|
| 1. SRI Horizontal Velocity Gage | 3 |
| 2. Model DX and Model DS Velocity Gage's. | 7 |
| 3. Exploded View of Horizontal Velocity Gage. | 11 |
| 4. Horizontal Velocity Gage Detail. | 12 |
| 5. Mechanical Actuating System. | 14 |
| 6. Approximated Pendulum. | 16 |
| 7. Pendulum's Mass Center Rotated to $\theta_{\max} = 12$ | 17 |
| 8. Pendulum's Mass Center Rotated to $\theta_{\max} = 12$ | 20 |
| 9. Front View of the Horizontal Velocity Gage | 22 |
| 10. Rectangular Channel. | 23 |
| 11. Pendulum Rotated to $\theta_{\max} = 12$ | 24 |
| 12. Apparent Coefficient C_{ap} | 32 |
| 13. Electrical and Magnetic Circuit. | 37 |
| 14. Oil Gap Distance l_{g1} , with $\theta(t) = 12$ | 45 |
| 15. Oil Gap Distance l_{g16} , with $\theta(t) = 12$ | 46 |
| 16. Equivalent Circuit | 47 |
| 17. E Core and Armature. | 51 |
| 18. Oscilloscope Picture of the Output Voltage | 57 |
| 19. Comparison of Experimental and Theoretical Output Peak Voltage for an Unforced System. | 58 |
| 20. Time for Maximum Deflection (t_{\max}), $v_1 = 500$ c.s. (Low Accelerations). | 60 |
| 21. Time for Maximum Deflection (t_{\max}), $v_1 = 500$ c.s. (High Accelerations) | 61 |
| 22. Time for Maximum Deflection (t_{\max}), $v_2 = 1,000$ c.s. (Low Accelerations). | 62 |
| 23. Time for Maximum Deflection (t_{\max}), $v_2 = 1,000$ c.s. (High Accelerations) | 63 |

| Figure | | Page |
|--------|--|------|
| 24. | Time for Maximum Deflection (t_{max}), $v_3 = 2,000$ c.s. (Low Acceleration) | 64 |
| 25. | Time for Maximum Deflection (t_{max}), $v_3 = 2,000$ c.s. (High Accelerations) | 65 |
| 26. | Input Acceleration Wave Form | 66 |
| 27. | Comparison of Normalized Velocity and Normalized Output Peak Voltage for 40 G's Peak Acceleration . . | 67 |
| 28. | Comparison of Normalized Velocity and Normalized Output Peak Voltage for 200 G's Peak Acceleration. . | 68 |
| 29. | Comparison of Normalized Velocity and Normalized Output Peak Voltage for 600 G's Peak Acceleration. . | 69 |

List of Tables

| Table | | Page |
|-------|--|------|
| I | C_{ap}, τ , and s Matrix | 33 |
| II | Generalized Damping, d_{ij} , Matrix. | 34 |
| III | K_{ij} Matrix. | 54 |
| IV | Break-Point Acceleration (A_{ij} in G's) and Times (t_{ij} in msec) | 59 |

List of SymbolsLatin Symbol

| | |
|--------------------|--|
| A | area, in m^2 |
| A_c | cross sectional area of the rectangular channel measured perpendicular to the flow, in m^2 |
| A_p | area of the plate of the pendulum, in m^2 |
| B | magnetic flux density, in weber/ m^2 |
| C_{ap} | apparent coefficient |
| D | generalized viscous damping force, having the units of momentum Kgm^2/sec^2 |
| D_e | equivalent diameter, in m |
| F | generalized applied force |
| F_D | force of oil acting on plate of the pendulum, in Kgm/sec^2 |
| g | force of gravity at a particular locality, in m/sec^2 |
| g_c | gravitational constant, has units of $32.174 \text{ lbm ft/lb}_f\text{sec}^2$ |
| H | magnetic field intensity, in amp/m |
| I_o | axial moment of inertia, in $Kg m^2$ |
| J | current density, in amp/m^2 |
| 2l | length from the pivot point to the end of the pendulum, in m |
| L | inductance, in henry |
| m | mass of the pendulum, in Kg |
| M | mass of the gage, in Kg |
| N | number of turns |
| P | pressure in $Kg/msec^2$ |
| Q | generalized force |
| q | generalized coordinate |
| R | reluctance, in amp-turn/weber |

Latin Symbol

| | |
|----------------------------|--|
| R | resistance, in ohms |
| Re | Reynolds number, dimensionless |
| T | kinetic energy, in joules |
| U | average velocity of the flow, in m/sec |
| V | potential energy, in joules |
| V | voltage, in volts, |
| V _{in} | voltage into the bridge circuit |
| V _{out} | voltage out of the bridge circuit |
| Vol | volume swept out by the plate of the pendulum, in m ³ |
| wd. | width of pendulum, in m |
| x | length of channel, in m |
| X | displacement of gage along the primary axis, in m |

Greek Symbol

| | |
|---------------------|--|
| δ | density constant |
| θ | angle of the pendulum from the center line of the gage, in radians |
| λ | flux linkage, in weber-turns |
| μ | absolute viscosity |
| μ | permeability, in henry/meter |
| ν | kinematic viscosity, in centistokes |
| ρ | density, in Kg/m ³ |
| γ | specific weight |
| ϕ | magnetic flux, in webers |
| ω | radian frequency, in rad/sec |

Abstract

A theoretical model of a Spartron Model 601M horizontal velocity gage is developed. The mechanical and electrical systems of the velocity gage are treated as separate entities and separate models of each system are developed. Lagrange's equations are used to develop the mechanical equation of motion. Ampere's circuital law is used to develop the inductance equations for the electrical model. The electrical system equations are developed by applying Kirchhoff's voltage law to an equivalent circuit for the bridge network. Then by defining state variables, the overall system equations are written. A Fortran program was developed to solve the overall system equations using a fourth order Runge-Kutta algorithm. The computer program is used to verify the overall system state model against a known laboratory result. Then results are shown which indicate the linear and non-linear operating ranges of the gage. Finally, results are shown which compare the gage output to the theoretical velocity for a known dynamic input.

THEORETICAL MODEL OF A
SPARTON MODEL 601M
HORIZONTAL VELOCITY GAGE

I. Introduction

Background Information

Since the late fifties much emphasis has been placed on protective structure design with the advent of underground missile complexes. Thus, free-field ground motion data, such as acceleration, particle velocities and displacement, became of specific interest. The first ground motion data resulted from underground nuclear explosions, as above ground nuclear tests were limited by the nuclear test ban treaty.

In the sixties work shifted to above ground High Explosive Simulation Technique (HEST) tests. In these tests above ground nuclear explosions were simulated using large amounts of TNT. Most recently the HEST tests have provided ground motion data for different types of soils for the hardening of the Minuteman II and III complexes.

The primary sensing device of all ground motion studies prior to 1960 and of many studies after that was the accelerometer. Rugged accelerometers were the only devices that could be obtained in adequate signal and frequency ranges to fulfill the requirements for the experiments planned. To acquire an adequate description of the transient ground motion it was necessary to determine particle velocity and/or displacement data. This data was obtained by integration of the acceleration records by analog or digital methods. Unfortunately, in this method any errors in the measurement of acceleration were

magnified greatly in the integration process.

Subsequently considerable effort was expended during the early sixties on the development and evaluation of a velocity gage that could be utilized with an underground nuclear or HEST test. The first model was designed and built by the British. It was based on the principle of a highly overdamped accelerometer. This instrument was a large self-recording meter having limited frequency response and operating range and employing magnetic damping.

Stanford Research Institute Velocity Gage. The Stanford Research Institute (SRI), Menlo Park, California, using the basic principle of the British model, developed a velocity gage for the Defense Atomic Support Agency. It was an overdamped, pendulum accelerometer with a carrier-excited variable-reluctance sensing element, externally completed as a standard AC-bridge circuit. Modulation of the bridge circuit was effected by an armature attached to a pendulum suspended from a shimstock hinge. Since the pendulum was flat in cross-section, the extreme damping was achieved by surrounding the pendulum with a highly viscous silicone oil. The pendulum displacement (and hence the bridge output) from the null point was proportional to the instantaneous velocity of the case within its linear operating range. A deflecting coil assembly which when energized would pull the pendulum off-scale to one side, served several purposes. When the gage was mounted for true horizontal measurement, energizing and then releasing this coil provided a record from which the low frequency time constant could be derived. For field calibration the coil was energized, the gage turned on its side, and a record was taken as the coil was released (1). Fig. 1 shows the configuration of the SRI horizontal

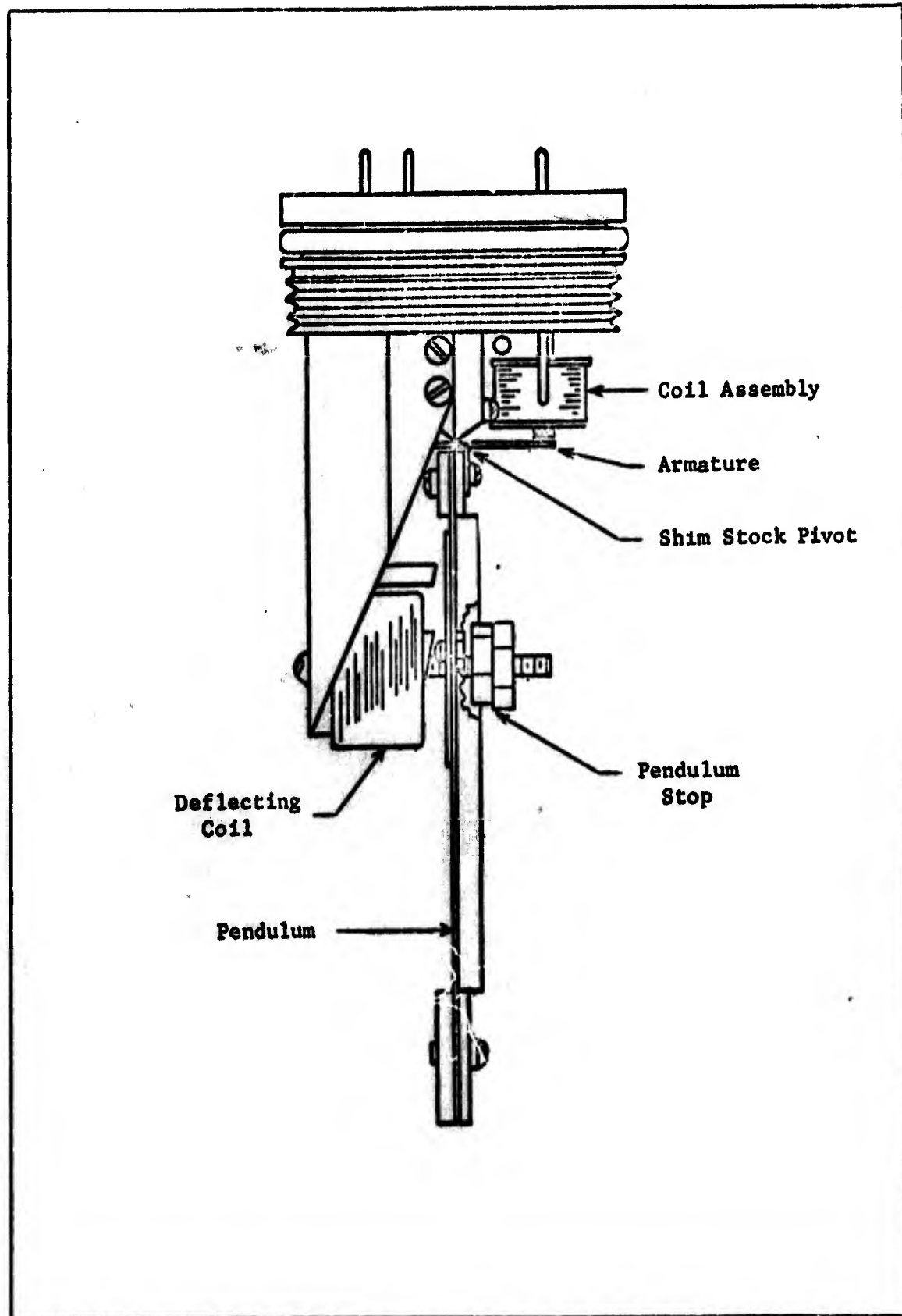


Fig. 1. SRI Horizontal Gage

velocity gage.

Sandia Corporation Velocity Gage. As information of the performance and limitations of the SRI velocity gages was acquired, several problem areas became apparent. In addition, much interest was expressed by hardened-structures people and other military agencies in extending the range of velocity measurements to close-in regions where accelerations were beyond the capabilities of the SRI gages (accelerations greater than 500 g). The Sandia Corporation of Albuquerque, New Mexico was given the responsibility of redesigning the SRI velocity gage. The design objectives for the Sandia velocity gage were (2):

1. To extend the gage frequency response to cover the range from 0.01Hz to 600Hz.
2. To extend the dynamic range of the gage to measure velocities from 0.1 ft/sec. to 600 ft/sec.
3. To strengthen the gage to withstand shock loads of at least 3000 g.
4. To investigate techniques of obtaining large values for the damping ratio without the necessity of using high viscosity damping fluids with possible thixotropic behavior. (Thixotropic fluids are shear dependent, i.e., their apparent viscosity decreases with increasing shear rate).
5. To extend the pendulum-reluctance pickoff linear operating range from $\pm 1.2^\circ$ to at least $\pm 4^\circ$.
6. To include a sealed expansion bellows to accommodate temperature expansion of the damping fluid.

7. To incorporate a method for filling the gages under a vacuum, to prevent air bubbles from forming in the fluid.

The first Sandia prototype was the Model DS velocity gage built and tested during the fall and winter of 1962. This model was used in 1963 and 1964 operations. The following major changes were incorporated into the redesign of the SRI gage (2):

1. The pendulum suspension system, the pendulum-armature-E coil assembly, and the gage body were completely redesigned and strengthened sufficiently to meet the 3000g shock requirement.
2. A miniature ballbearing and pivot assembly was substituted for the shimstock hinge which was found to be incompatible with high "g" operation.
3. The variable reluctance sensor as used in the SRI gage was retained, but the linear operating range of the gage was doubled by increasing the armature gap.
4. To avoid possible problems associated with air entrapment in the damping fluid, a system for filling the gages with damping fluid under a moderate vacuum and for subsequent sealing was devised.
5. Temperature expansion of the damping fluid was accommodated by a flexible bellows, decoupled from the pendulum working chamber by an orifice plate containing a small diameter bleed hole.
6. The standard DS gage was provided with a brass pendulum and was used to measure velocities in the range of 0.1 ft/sec. to 25 ft/sec. (A higher "g" version of this gage

had an aluminum pendulum and measured velocities between 5 ft/sec. and 300 ft/sec.)

Further experimentation and redesign produced the Sandia Model DX velocity gage which replaced the DS Model. This model was first used in 1964 operations. Fig. 2 shows an exploded view of the DX velocity gage. The major change was in redesigning the damping system. The Model DS velocity gage required damping fluid viscosities above a few thousand centistokes to provide the necessary high damping ratios. It was found that damping fluids with viscosities greater than a few thousand centistokes behaved increasingly as thixotropic fluids rather than simple Newtonian fluids (2). This implied that at certain shear rates, and therefore at certain pendulum velocities abnormal gage response could be expected. Thus, it was desired to increase the effective damping available for any given viscous fluid, since lower viscosity fluids have a higher critical shear rate. This was accomplished by designing a close tolerance gap between the pendulum and the pendulum housing. This detail is illustrated in Fig. 2. The effective damping ratio (for any given fluid viscosity) was increased by a factor of approximately four. Other improvements incorporated into this design were (2):

1. An improved pivot and bearing assembly which decreased the friction in the pendulum suspension system and extended the gage operating limit into the 3000 g region.
2. The armature gap was increased to provide linear operation over $\pm 4^\circ$ pendulum rotation. Maximum pendulum rotation was $\pm 6.5^\circ$. This gap change extended the velocity measuring capability of the gage to about 600 ft/sec.

3. DX gages with brass pendulums covered the velocity range of 0.1 ft/sec. to 50 ft/sec. Those with aluminum pendulums operated in the range of 5 ft/sec. to 600 ft/sec.

Both the Model DS and the Model DX velocity gages were converted to vertical operation by supporting the pendulum in the horizontal plane by means of a "soft" coil spring which just counteracted the earth's gravitational field.

Sparton Model 601 Velocity Gage. The Sandia Model DX velocity gage is being commercially manufactured by Sparton Southwest Inc., Albuquerque, New Mexico, as the Sparton Model 601 velocity gage. In the Sparton Model 601M the armature has been shortened to allow a maximum pendulum rotation of $\pm 12^\circ$.

Statement of the Problem

The general problem upon which this thesis is based can be stated as follows:

To develop a theoretical model of the Sparton Model 601M horizontal velocity gage with a brass pendulum.

This problem was presented by the Chief of the Experimental Branch of the Civil Engineering Research Division, Air Force Weapons Laboratory, Kirtland Air Force Base, New Mexico. This branch is conducting ground motion studies in conjunction with HEST tests in different types of soils for the hardening of the Minuteman II and III complexes. Since a theoretical model of the gage does not exist, they are interested in acquiring one for the following reasons:

1. to lend insight into the operation of the gage.
2. to help establish what the linear operating range of the gage is for soils with different viscosities.

Scope of the Investigation

To accomplish the above-mentioned objective, the mechanical and electrical systems of the velocity gage were treated as separate entities and separate models of each system were developed. Lagrange's equations were used to develop the mechanical equation describing the motion of the pendulum with an excitation force applied to the gage. Ampere's circuital law was used to develop the inductance equations for the electrical model. The electrical system equations were developed by applying Kirchhoff's voltage law to an equivalent circuit for the bridge network. Then by defining state variables, the overall system equations were written. A Fortran program was developed to solve the overall system equations using a fourth order Runge-Kutta algorithm.

In Chapter II the model development of the gage is presented. A word description of the horizontal velocity gage is presented, followed by the development of a mechanical model. Next the electrical model is developed. Finally the overall system state model is presented. Chapter III deals with the computer simulation of the overall system equations. A description of the computer program is presented. A comparison of the results obtained from the computer solution of the overall system equations to a known laboratory result is presented. Results are shown which indicate the linear operating range of the gage for different viscous oils. Finally results are shown for several dynamic causes which illustrate the various regions of operation. The conclusions reached and some recommendations for future work are contained in Chapter IV.

There are two appendices in the thesis. Appendix A-Computer Program Symbols-relates the symbols used in the program to symbols used in the model. Appendix B-Computer Program Listing-presents a listing of the program.

II. The Analytical Model

Word Description of the Velocity Gage

The Sparton Model 601M horizontal velocity gage is an overdamped, pendulum accelerometer with a carrier-excited variable-reluctance sensing element, externally completed as a standard AC-bridge circuit. Modulation of the bridge circuit is effected by an armature attached to the pendulum. The pendulum displacement (and hence, the bridge output) from the null point is proportional to the instantaneous velocity of the case within a given spectrum (dependent on the fluid viscosity or degree of damping). An exploded view of the horizontal velocity gage is shown in Fig. 3.

The horizontal velocity gage is shown in detail in Fig. 4. It consists of a mechanical actuating and an electrical sensing system. The actuating element is the pendulum, which hangs from a pivot and bearing assembly. The sensing element of the gage consists of two coils, an E core, and an armature (top of pendulum) which make up an inductance path when the coils are excited. The E core, the armature, and the oil gap between them have a certain reluctance value. As the pendulum swings, the oil gap in the path for each coil changes. This changes the reluctance for each coil, and consequently changes the inductance of each coil. This change in inductance produces an imbalance between the two coils. This imbalance is the output signal of the gage. The two coils are electrically connected with two 315 ohm resistors to form a bridge. The bridge is balanced (zero output) when the pendulum hangs perpendicular to the top of the gage. The input to the bridge is a 3KHz, 10 volt RMS sine wave.

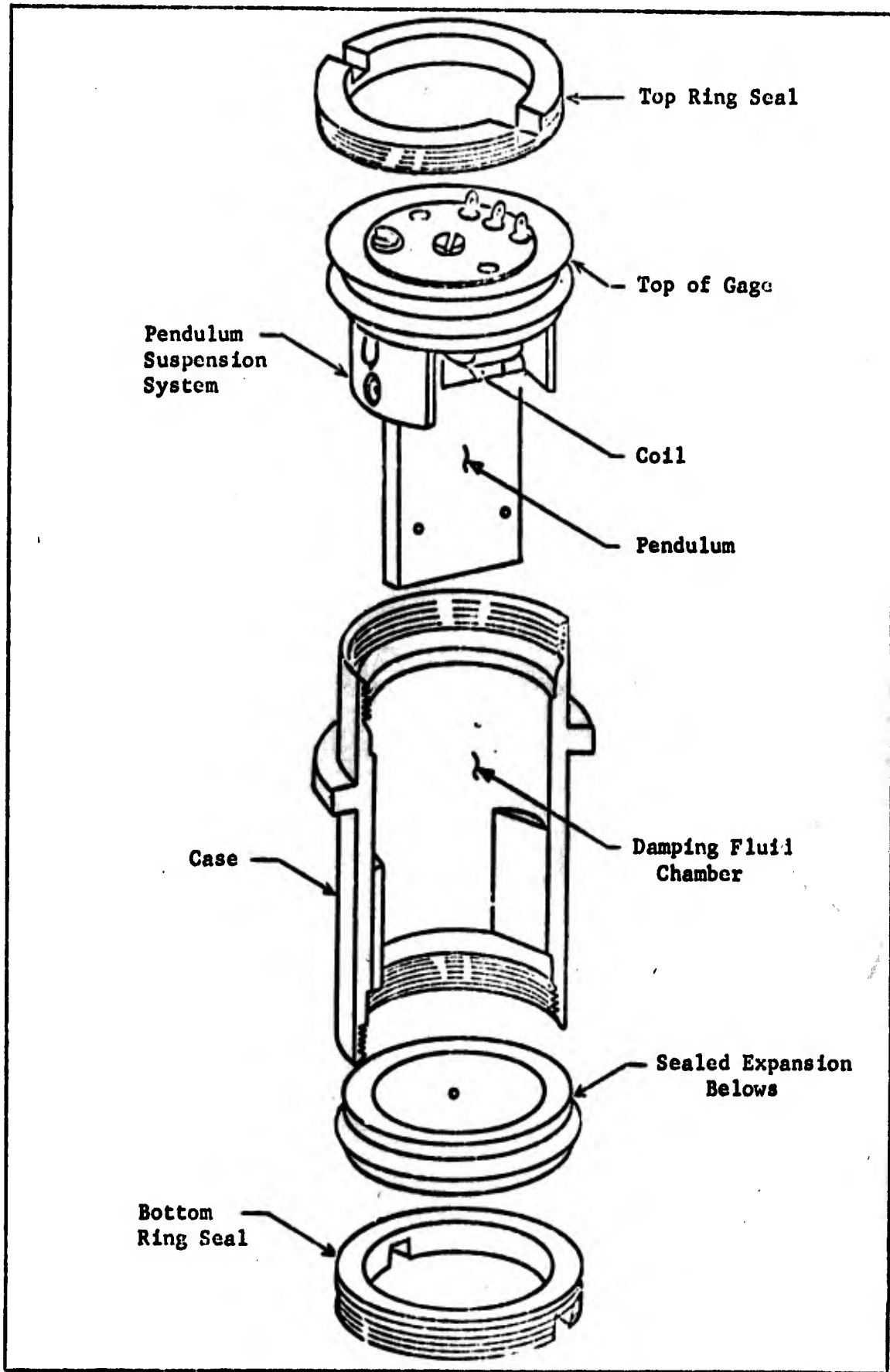
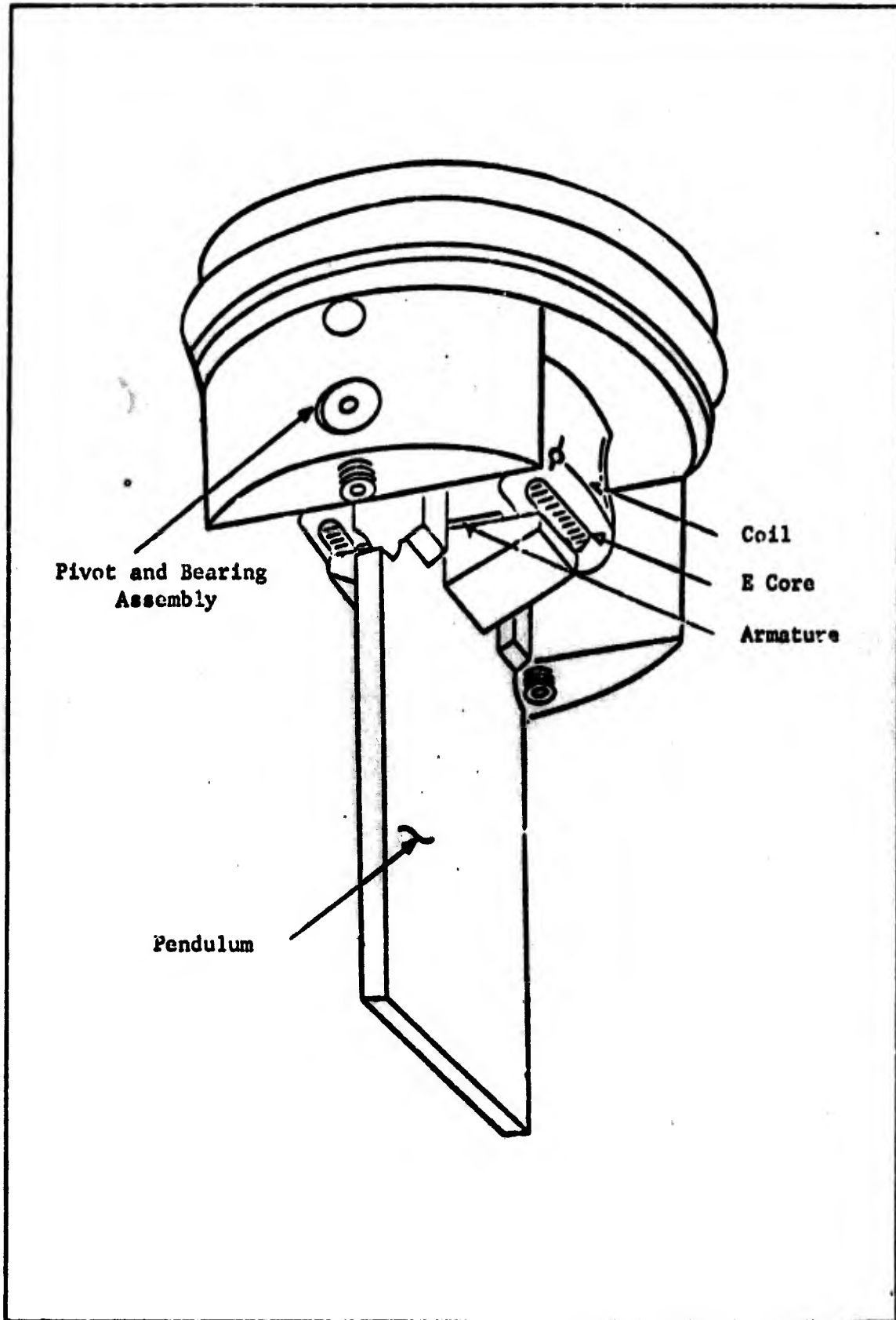


Fig. 3. Exploded View of Horizontal Velocity Gage



Pivot and Bearing
Assembly

Pendulum

Coil
E Core
Armature

Fig. 4. Horizontal Velocity Gage Detail

The mechanical and electrical systems of the velocity gage can be treated as separate systems if the small magnetic-attraction forces are neglected. Thus, the analysis of each system was performed separately.

Mechanical Model

Lagrange's equations were used to develop the mechanical equation of motion in a manner similar to that in reference 3. In the referenced report a theoretical method for calculating the damping effect of the oil on the pendulum was not developed. In this study considerable research was done to develop such a method. The most general form of Lagrange's equations can be written as (4).

$$\frac{d}{dt} \frac{\partial T(q_i, \dot{q}_i)}{\partial \dot{q}_i} - \frac{\partial T(q_i, \dot{q}_i)}{\partial q_i} = Q_i, \quad i = 1, 2, \dots \quad (1)$$

Where

T is the total kinetic energy of the system

q_i is a generalized coordinate

$\dot{q}_i = \frac{dq_i}{dt}$ (generalized velocity)

Q_i are the generalized forces at the coordinate i

For a simple conservative system the generalized forces are derived from the potential energy, V , that is

$$Q_i = - \frac{\partial V(q_i)}{\partial q_i} \quad (2)$$

The function is negative for it results from work done by the system.

This system is nonconservative since the pendulum is damped by a highly viscous silicone oil which dissipates energy. For such a

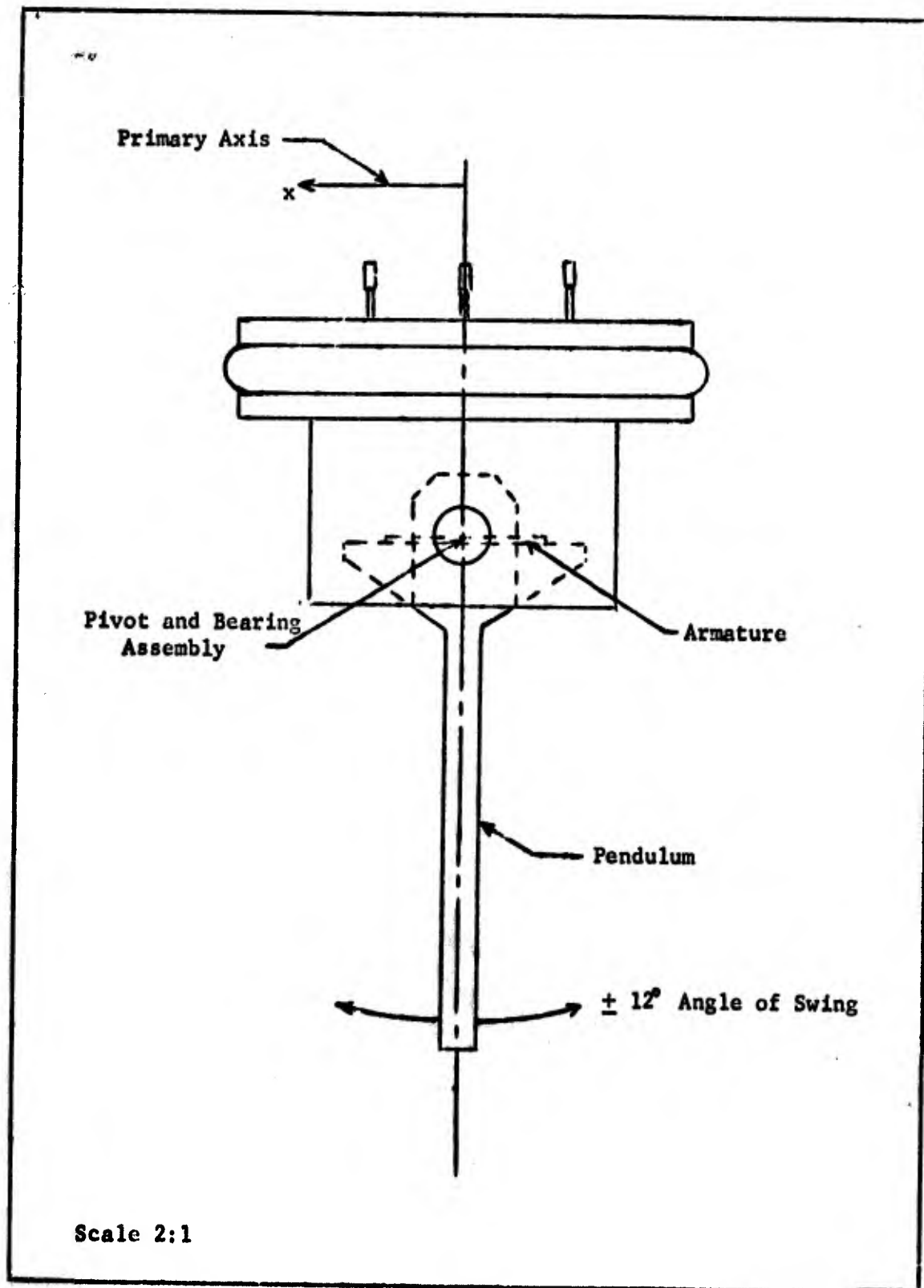


Fig. 5. Mechanical Actuating System

system the generalized forces, Q_i , are usually separated into the following three components (4)

$$Q_i = - \frac{\partial V(q_i)}{\partial q_i} - D_i + F_i \quad (3)$$

Where

$\frac{\partial V(q_i)}{\partial q_i}$ is the generalized force derived from the potential energy.

D_i is a generalized damping force, and is also negative for it results from work done by the system.

F_i is the generalized applied force, and is positive for it results from work done to the system.

Fig. 5 shows the mechanical actuating system. The excitation force is considered to be applied to the gage only along the primary axis (i.e. the x axis). Let

m = mass of the pendulum

M = mass of the gage

$2l$ = length from the pivot point to the end of the pendulum

$\theta(t)$ = angle of the pendulum from the center line of the gage as a function of time (positive in ccw direction).

$\dot{\theta}(t) = \frac{d\theta(t)}{dt}$ = angular velocity

$X(t)$ = displacement of gage along the primary axis as a function of time

$\dot{X}(t) = \frac{dX(t)}{dt}$ = displacement velocity

Kinetic Energy of the System. The kinetic energy of this system can be calculated by the Theorem of Konig (5). The theorem of Konig states, "The kinetic energy of a moving system is equal to the sum of

(1) the kinetic energy of a fictitious particle moving with the mass center and having a mass equal to the total mass of the system and (2) the kinetic energy of the motion relative to the mass center." By this theorem the kinetic energy of the gage is composed of

(1) the kinetic energy of a fictitious particle moving with the pendulum's mass center and having a mass equal to the total mass of the pendulum, and the kinetic energy of a fictitious particle moving with the gage's mass center and having a mass equal to the total mass of the gage.

(2) the kinetic energy of the motion of the pendulum relative to its mass center.

Let the pendulum be approximated by the rectangular pendulum shown in Fig. 6.

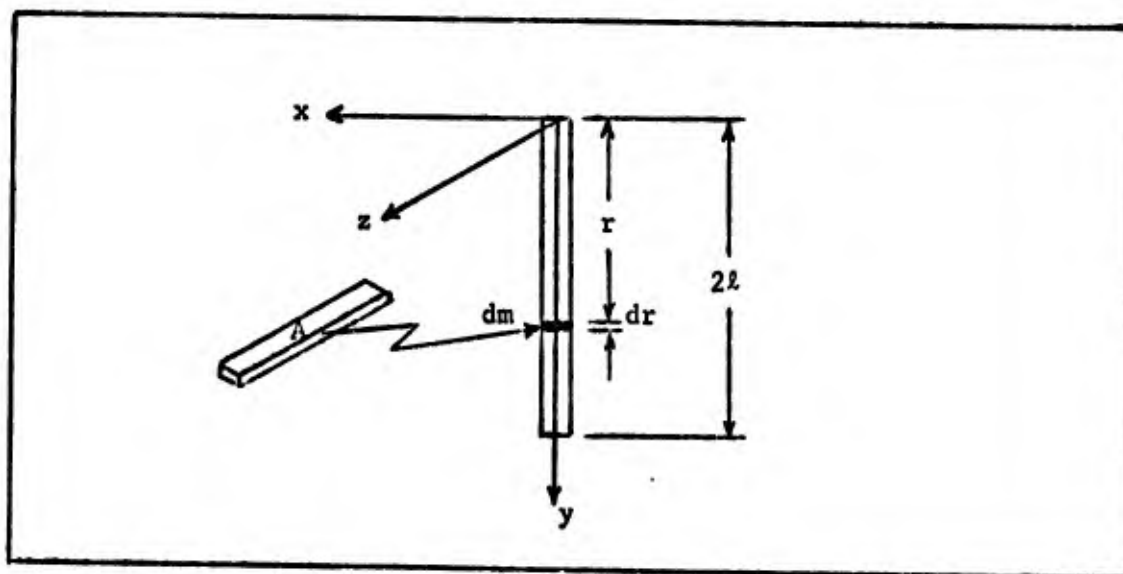


Fig. 6. Approximated Pendulum

The axis of rotation is the z axis. Since the pendulum is a homogeneous mass the centroid (i.e. the distance from the axis of rotation to the center of mass) can be written as

$$\bar{r} = \frac{\int_0^{2l} r dm}{\int_0^{2l} dm} \quad (4)$$

The increment of mass dm can be written as

$$dm = \delta dV = \delta A dr \quad (5)$$

where

δ = density constant

Substituting Eq (5) into Eq (4) yields

$$\bar{r} = \frac{\int_0^{2l} r \delta A dr}{\int_0^{2l} \delta A dr} \quad (6)$$

Performing the integration yields

$$\bar{r} = l \quad (7)$$

With an excitation force applied to the gage along the x axis the pendulum's mass center will rotate as shown in Fig. 7.

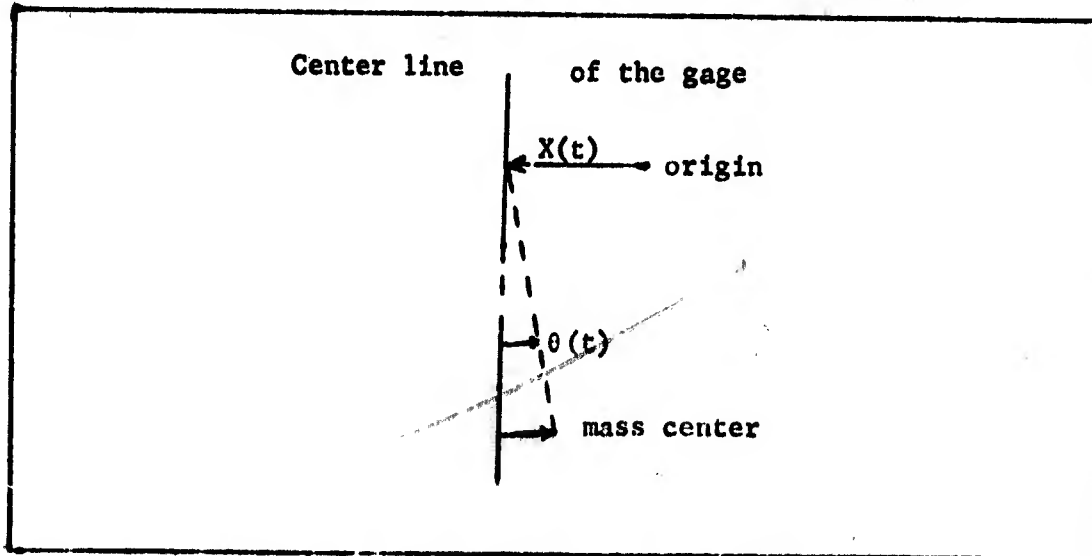


Fig. 7. Pendulum's Mass Center Rotated to $\theta_{\max} = 12^\circ$

Since $X(t)$ is the displacement of the gage along the x axis the pendulum's mass center will have to move approximately a distance of

$$X(t) - 2\theta(t) \quad (8)$$

Then the kinetic energy of a fictitious particle moving with the mass center of the pendulum and having a mass equal to the total mass of the pendulum is

$$T_1 = \frac{1}{2} m \left[\dot{X}(t) - 2\dot{\theta}(t) \right]^2 \quad (9)$$

Because of symmetry the gage's mass center can be assumed to lie on the center line of the gage. The kinetic energy of a fictitious particle moving with the gage's mass center and having a mass equal to the total mass of the gage is

$$T_2 = \frac{1}{2} M \dot{X}(t)^2 \quad (10)$$

The kinetic energy of the motion of the pendulum relative to its mass center, is (5)

$$T_3 = \frac{1}{2} I_0 \dot{\theta}(t)^2 \quad (11)$$

The moment of inertia with respect to mass center of the pendulum, can be expressed mathematically as

$$T_0 = \int_{-l}^l r^2 dm \quad (12)$$

Substituting Eq (5) into Eq (12) yields

$$I_o = \int_{-l}^l r^2 \delta A dr \quad (13)$$

Performing the integration yields

$$I_o = m \frac{l^2}{3} \quad (14)$$

where $m = 2l\delta A$.

Substituting Eq (14) into Eq (11), the kinetic energy of the motion of the pendulum relative to its mass center is

$$T_3 = m \frac{l^2}{6} \dot{\theta}(t)^2 \quad (15)$$

The total kinetic energy, T , of the gage is $T_1 + T_2 + T_3$, that is

$$T = \frac{1}{2} m [\dot{X}(t) - l\dot{\theta}(t)]^2 + \frac{1}{2} M\dot{X}(t)^2 + m \frac{l^2}{6} \dot{\theta}(t)^2 \quad (16)$$

Performing the multiplication and collecting like terms yields

$$T = \frac{1}{2} m\dot{X}(t)^2 - m\dot{X}(t)l\dot{\theta}(t) + \frac{2}{3} ml^2\dot{\theta}(t)^2 + \frac{1}{2} M\dot{X}(t)^2 \quad (17)$$

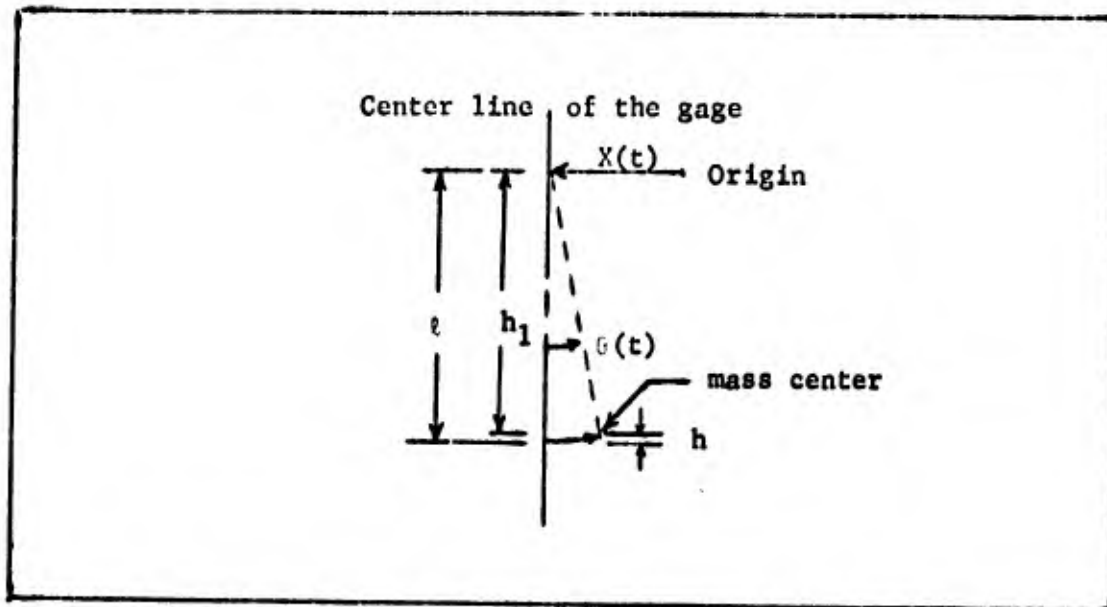
Potential Energy of the System.

Fig. 8. Pendulum's Mass Center Rotated to $\theta_{\max} = 12$

Fig. 8 again shows the rotation of the pendulum's mass center, as an excitation force is applied to the gage along the x axis. The potential energy, V , of the gage is the inherent energy due to the position of the pendulum with respect to its original vertical position. Since the potential energy of a body is equal to that of a single particle with a mass equal to the total mass of the body situated at the mass center, raising the mass center through a distance of h , where g is the acceleration due to gravity yields

$$V = mgh \quad (18)$$

Referring to Fig. 8, h can be written as

$$h = l - h_1 \quad (19)$$

or

$$h = l(1 - \cos\theta(t)) \quad (20)$$

Substituting Eq (20) into Eq (18) the potential energy of the gage can be written as

$$V = mgl(1 - \cos\theta(t)) \quad (21)$$

Generalized Viscous Damping Force. The generalized damping force is a moment caused by the highly viscous silicone oil acting on the pendulum. As an excitation force is applied to the gage the pendulum will rotate causing an oil flow through the close tolerance opening between the pendulum and the pendulum housing. See Fig. 9. This opening is shown in Fig. 10, as a three dimensional rectangular channel. For this model it is assumed that all oil flows through this channel (i.e. flow at the top of the gage will be neglected).

The nature of the flow (i.e. whether it is laminar or turbulent) is indicated by a Reynolds number. Laminar (viscous) flow is defined as flow in which the fluid moves in layers, or laminae, one layer gliding smoothly over an adjacent layer with only a molecular interchange of momentum. Turbulent flow, however; has very erratic motion of fluid particles, with a violent transverse interchange of momentum. The Reynolds number is a dimensionless expression made up of a group of variables which depend on the rate of flow, the properties of the fluid, and the geometry of the device containing the fluid flow. Laminar flow is indicated by low values of Reynolds number. Turbulent

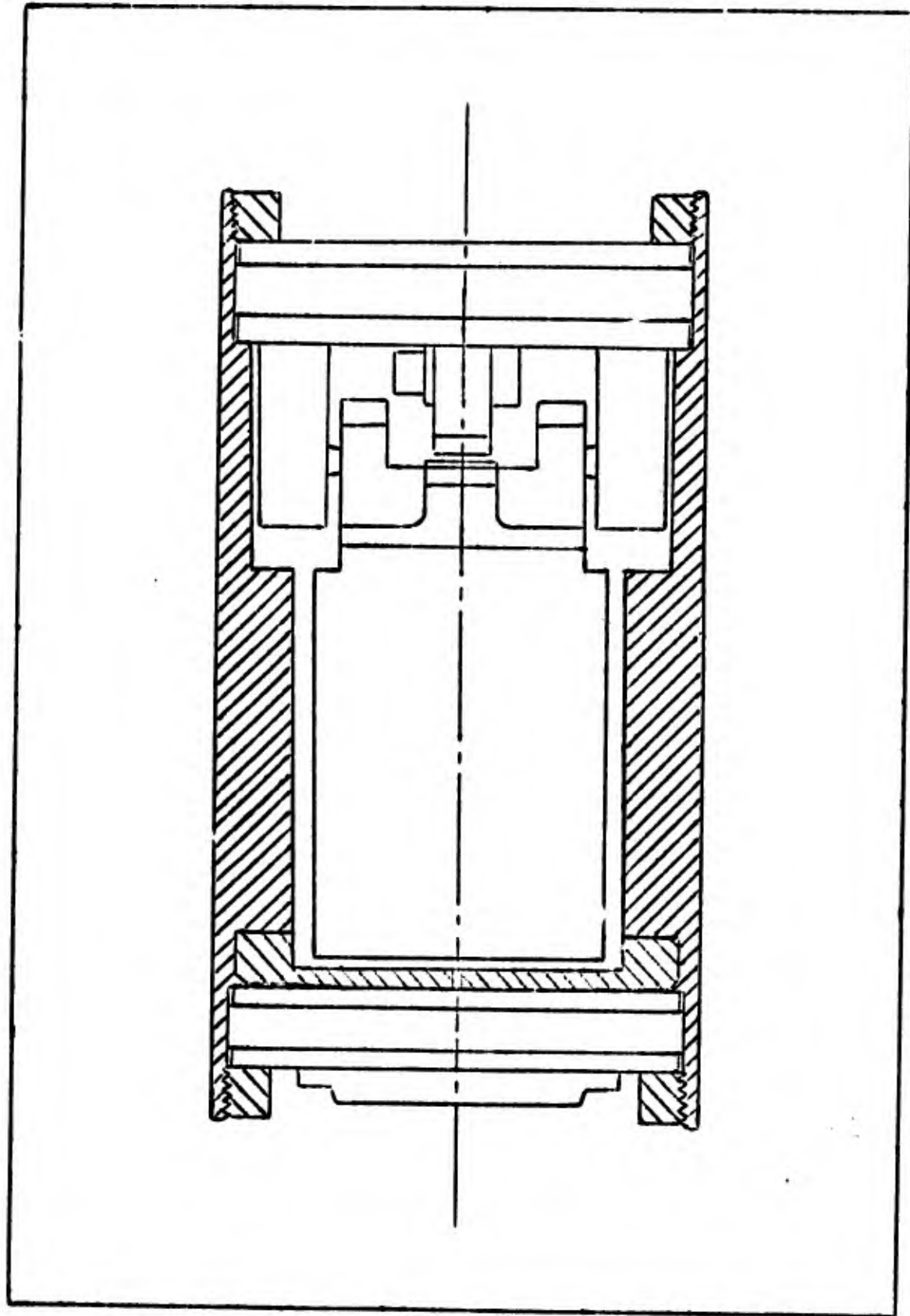


Fig. 9. Front View of the Horizontal Velocity Gage

flow is indicated by high values of Reynolds number. In rectangular channels the transition from one type of flow to another usually begins at a Reynolds number of between 1,500 and 2,300, with a value of 1,800 being recommended as representative (6). The Reynolds number is given by the following equation (6,7):

$$R_e = \frac{UD_e}{\nu} \quad (22)$$

where

U = average velocity of the flow

ν = kinematic viscosity of the fluid

D_e = equivalent diameter

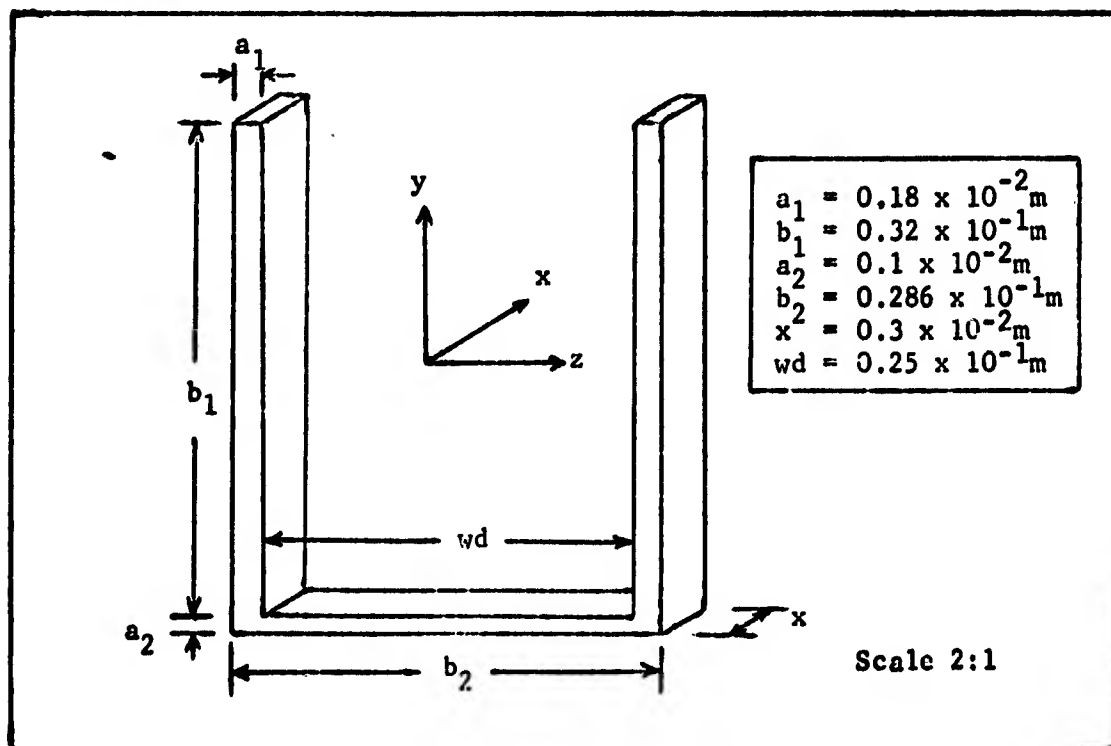


Fig. 10. The Rectangular Channel

The average velocity of the flow in the rectangular channel is

$$U = \frac{\frac{dVol(t)}{dt}}{I_c} \quad (23)$$

where

$\frac{d \text{Vol}(t)}{dt}$ = the time rate of change of the volume swept out by the plate of the pendulum, which is the flow rate through the rectangular channel.

A_c = cross sectional area of the rectangular channel measured perpendicular to the flow.

The volume swept out by the plate of the pendulum as shown in Fig. 11.

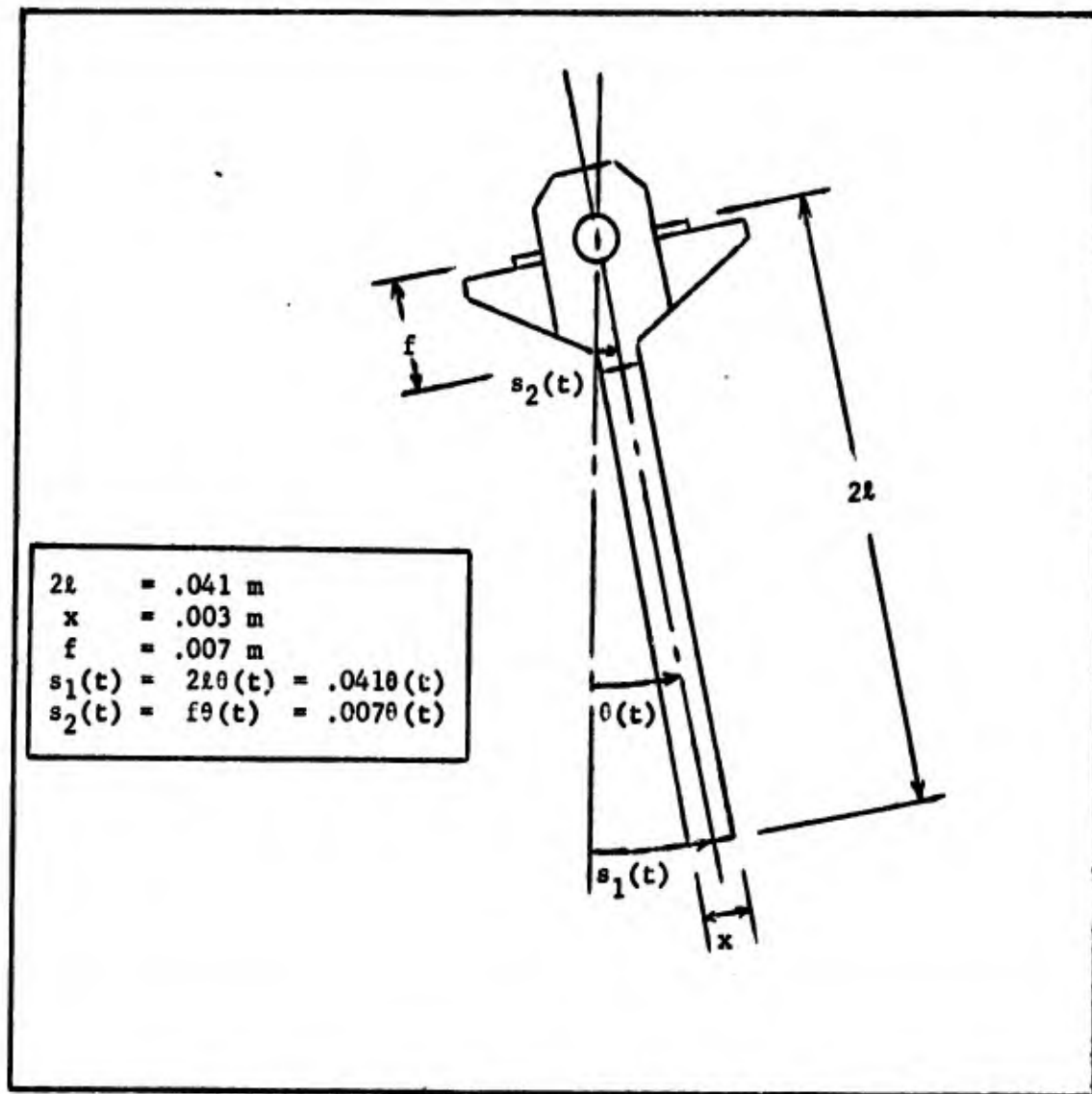


Fig. 11. Pendulum Rotated to $\theta_{\max} = 12^\circ$

The volume swept out can be written as

$$\text{Vol}(t) = \frac{1}{2} S_1(t)(2\ell)(wd) - \frac{1}{2} S_2(t)(f)(wd) \quad (24a)$$

$$\text{Vol}(t) = 0.204 \times 10^{-4} \theta(t) m^3 \quad (24b)$$

Then

$$\frac{d \text{Vol}(t)}{dt} = 0.204 \times 10^{-4} \dot{\theta}(t) \frac{m^3}{\text{sec}} \quad (25)$$

The cross-sectional area of the rectangular channel as shown in Fig. 10 is

$$A_c = 2(a_1)(b_1) + a_2 b_2 = 0.1438 \times 10^{-3} m^2 \quad (26)$$

Substituting Eq's (25) and (26) into Eq (23) the average velocity of flo. in the rectangular channel is

$$U = 0.1418636 \dot{\theta}(t) \frac{m}{\text{sec}} \quad (27)$$

The equivalent diameter for a rectangular channel is defined as four times the cross-sectional area divided by the wetted perimeter, both being measured perpendicular to the flow (6,7). Thus

$$D_e = \frac{4A_c}{\text{Perimeter}} \quad (28)$$

Referring to Fig. 10 the wetted perimeter can be written as

$$\text{Perimeter} = 4b_1 + 2a_2 + 2b_2 = 0.1872m \quad (29)$$

Substituting Eq's (26) and (29) into Eq (28) the equivalent diameter can be written as

$$D_e = 0.30726 \times 10^{-2} m \quad (30)$$

The kinematic viscosity, ν , is given in units of cm^2/sec , which is referred to as a stoke. A smaller unit called the centistoke is 1/100 of a stoke. Converting to the mks system yields

$$\text{centistoke} = 10^{-6} \frac{\text{m}^2}{\text{sec}} \quad (31)$$

Three different oils are considered in this model, corresponding to the kinematic viscosities of 500, 1,000, and 2,000 centistokes. Using Eq (31) to convert the kinematic viscosities to the mks system yields

$$\nu_1 = 500 \text{ centistokes} = 5 \times 10^{-3} \frac{\text{m}^2}{\text{sec}} \quad (32a)$$

$$\nu_2 = 1000 \text{ centistokes} = 1 \times 10^{-2} \frac{\text{m}^2}{\text{sec}} \quad (32b)$$

$$\nu_3 = 2000 \text{ centistokes} = 2 \times 10^{-2} \frac{\text{m}^2}{\text{sec}} \quad (32c)$$

Substituting Eq's (27), (30), and (32) into Eq (22), the Reynolds number for the different viscous oils can be written as $Re = K_{Re} |\dot{\theta}(t)|$.

That is

$$R_e = 0.817178 |\dot{\theta}(t)|, \text{ For 500 centistokes} \quad (33a)$$

$$R_e = 0.43589 |\dot{\theta}(t)|, \text{ For 1000 centistokes} \quad (33b)$$

$$R_e = 0.21795 |\dot{\theta}(t)|, \text{ For 2000 centistokes} \quad (33c)$$

Thus, it can be concluded that there is laminar flow in the rectangular channel for very high values of $\dot{\theta}(t)$.

Navier-Stokes equations for the motion of a viscous incompressible fluid can now be applied since it has been established that there is laminar (viscous) flow in the rectangular channel. These equations in Cartesian coordinates are as follows (8):

$$\rho \frac{Du}{Dt} = \rho X - \frac{\partial P}{\partial x} + \mu \left(\frac{\partial^2 u}{\partial x^2} + \frac{\partial^2 u}{\partial y^2} + \frac{\partial^2 u}{\partial z^2} \right) \quad (34a)$$

$$\rho \frac{Dv}{Dt} = Y - \frac{\partial P}{\partial y} + \mu \left(\frac{\partial^2 v}{\partial x^2} + \frac{\partial^2 v}{\partial y^2} + \frac{\partial^2 v}{\partial z^2} \right) \quad (34b)$$

$$\rho \frac{Dw}{Dt} = Z - \frac{\partial P}{\partial z} + \mu \left(\frac{\partial^2 w}{\partial x^2} + \frac{\partial^2 w}{\partial y^2} + \frac{\partial^2 w}{\partial z^2} \right) \quad (34c)$$

where the operator D/Dt means

$$\frac{D}{Dt} = \frac{\partial}{\partial t} + u \frac{\partial}{\partial x} + v \frac{\partial}{\partial y} + w \frac{\partial}{\partial z}$$

and

μ = absolute viscosity

ρ = density (and is a constant)

$P = P(x, y, z, t)$ is the pressure

$u = f_1(x, y, z, t)$ is the x component of velocity

$v = f_2(x, y, z, t)$ is the y component of velocity

$w = f_3(x, y, z, t)$ is the z component of velocity

X , Y , and Z are the x , y , and z components of body forces per unit volume respectively.

A research of the literature was performed to obtain previously published work done on solutions of Navier-Stokes equations when applied to rectangular channels of ducts. For laminar flow between a pair of parallel and infinite plates developing flow solution was obtained in 1934 by Schlichting (9). Additional work was done in 1960 by Han (7). If some approximations are assumed for this model, Han's results can be extended for use in this problem. The first approximation, referring to Fig. 10, is to assume that the flow velocities v and w along the y and z axis respectively can be neglected, for they are small compared to the velocity u along the x axis. Then assume that the viscous fluid enters all portions of the rectangular channel

at some average velocity in the x direction so the $\partial u/\partial y$ and the $\partial u/\partial z$ are zero. Furthermore, as Han points out, the usual boundary-layer analysis assumes a small region close to the duct wall in which the shearing stress is large. This leads to the conclusion that $\partial^2 u/\partial x^2$ may be dropped in comparison with $\partial^2 u/\partial y^2$ and $\partial^2 u/\partial z^2$. Using these approximations and assuming that the body forces are zero, Eq's (34) reduce to

$$\frac{\partial u}{\partial t} + u \frac{\partial u}{\partial x} = - \frac{1}{\rho} \frac{\partial P}{\partial x} + \nu \left(\frac{\partial^2 u}{\partial y^2} + \frac{\partial^2 u}{\partial z^2} \right) \quad (35a)$$

and

$$0 = - \frac{\partial P}{\partial y} \quad , \quad 0 = - \frac{\partial P}{\partial z} \quad (35b)$$

Consequently, pressure is a function of x and t only. For a constant input velocity, the equation reduces to

$$u \frac{\partial u}{\partial x} = - \frac{1}{\rho} \frac{\partial P}{\partial x} + \nu \left(\frac{\partial^2 u}{\partial y^2} + \frac{\partial^2 u}{\partial z^2} \right) \quad (36)$$

This equation was solved by Han for the pressure drop across a channel. His solution is given by

$$\Delta P = \left(\frac{C_{ap}}{R_e} \right) \left(\frac{x}{D_e} \right) \left(\frac{\rho U^2}{2} \right) \quad (37)$$

where

C_{ap} = apparent coefficient

x = length of channel

Han has given the apparent coefficient, C_{ap} , as a curve for a wide range of values of $x/D_e R_e$ (see Fig. 12 on page 32). In this problem the Reynolds number is a function of $\dot{\theta}(t)$ (see Eq's (33)), thus C_{ap} is a function of $\dot{\theta}(t)$. A general approximation to the curve shown in Fig. 12. Han's solution is applied to this time varying problem by

using the general equation for C_{ap} , to solve for a new C_{ap} every time $\dot{\theta}(t)$ changes value. The average entrance velocity, U , is given by Eq (27), the Reynolds numbers, R_e , by Eq's (33), the equivalent diameter, D_e , by Eq (30), and referring to Fig. 10 the length of channel, x , is 0.003m. The density of the oil, ρ , will have to be calculated.

The density can be calculated if the specific gravity is known. The specific gravity of a substance is defined as the ratio of its density (or specific weight) to that of pure water. The specific weight, γ , is defined as weight per unit volume and can be written as (10)

$$\gamma = \frac{\rho g}{g_c} \quad (38)$$

where

g = force of gravity at a particular locality

g_c = gravitational constant having the magnitude and units of

$$32.174 \frac{\text{ft}}{\text{sec}^2} \frac{\text{lbm}}{\text{lb}_f}$$

A specific gravity of 0.971 is given for the three oils used in this model at a temperature of 25°C (11). That is

$$0.971 = \frac{\gamma_{\text{oil at } 25^\circ\text{C}}}{\gamma_{\text{water at } 25^\circ\text{C}}} = \frac{\rho_{\text{oil at } 25^\circ\text{C}}}{\rho_{\text{water at } 25^\circ\text{C}}} \quad (39)$$

Solving Eq (39) for the density of the oil at a temperature of 25°C yields

$$\rho_{\text{oil at } 25^\circ\text{C}} = 0.971 \rho_{\text{water at } 25^\circ\text{C}} \quad (40)$$

Solving Eq (38) for the density yields

$$\rho = \frac{\gamma g_c}{g} \quad (41)$$

At sea level $g = 32.174 \text{ ft/sec}^2$, and specific weight, γ , of water at 25° is $62.24 \frac{\text{lb}_f}{\text{ft}^3}$ (12). Substituting these values into Eq (41), the density of water at sea level and a temperature of 25°C can be written as

$$\rho_{\text{water at } 25^\circ\text{C}} = 62.24 \frac{\text{lb}_m}{\text{ft}^3} \quad (42)$$

Substituting Eq (42) into Eq (40) the density of the three oils at sea level and a temperature of 25°C can be written as

$$\rho = 60.435 \frac{\text{lb}_m}{\text{ft}^3} \quad (43)$$

Converting, ρ , to the mks system where $\text{lb}_m = 0.45359 \text{ Kg}$ and $\text{ft} = 0.3048\text{m}$ yields

$$\rho = 968.08 \frac{\text{Kg}}{\text{m}^3} \quad (44)$$

Substituting Eq's (27), (30), (33), and (44), and the value for x into Eq (32), the pressure drops for the oils can be written as

$$\Delta P = C_{ap} (10.413) \dot{\theta}(t) \frac{\text{Kg}}{\text{m sec}^2}, \text{ For 500 centistokes} \quad (45a)$$

$$\Delta P = C_{ap} (21.820) \dot{\theta}(t) \frac{\text{Kg}}{\text{m sec}^2}, \text{ For 1000 centistokes} \quad (45b)$$

$$\Delta P = C_{ap} (41.654) \dot{\theta}(t) \frac{\text{Kg}}{\text{m sec}^2}, \text{ For 2000 centistokes} \quad (45c)$$

The force of the oil acting on the pendulum is

$$F_o = \Delta P A_p \quad (46)$$

Where A_p is the area of the plate of the pendulum and, referring to Fig's. 10 and 11, can be written as

$$A_p = (wd)(2l - f) = 0.85 \times 10^{-3} \text{m}^2 \quad (47)$$

Substituting Eq's (45) and (47) into Eq (46), the force of the oil acting on the pendulum for the three different viscous oils can be written as

$$F_D = C_{ap}(0.8851 \times 10^{-2})\dot{\theta}(t) \frac{\text{Kgm}}{\text{sec}^2}, \text{ For 500 centistokes} \quad (48a)$$

$$F_D = C_{ap}(0.18547 \times 10^{-1})\dot{\theta}(t) \frac{\text{Kgm}}{\text{sec}^2}, \text{ For 1000 centistokes} \quad (48b)$$

$$F_D = C_{ap}(0.35406 \times 10^{-1})\dot{\theta}(t) \frac{\text{Kgm}}{\text{sec}^2}, \text{ For 2000 centistokes} \quad (48c)$$

The generalized viscous damping force, D , in Eq (3) is a moment caused by the force of the oil acting on the pendulum. The moment arm is the length from the pivotal axis to the point where the flow is average (i.e. the point where the volume of oil swept out above this point is equal to the volume of oil swept out below this point) and is approximately $4l/3$. Thus the generalized viscous damping force can be written as

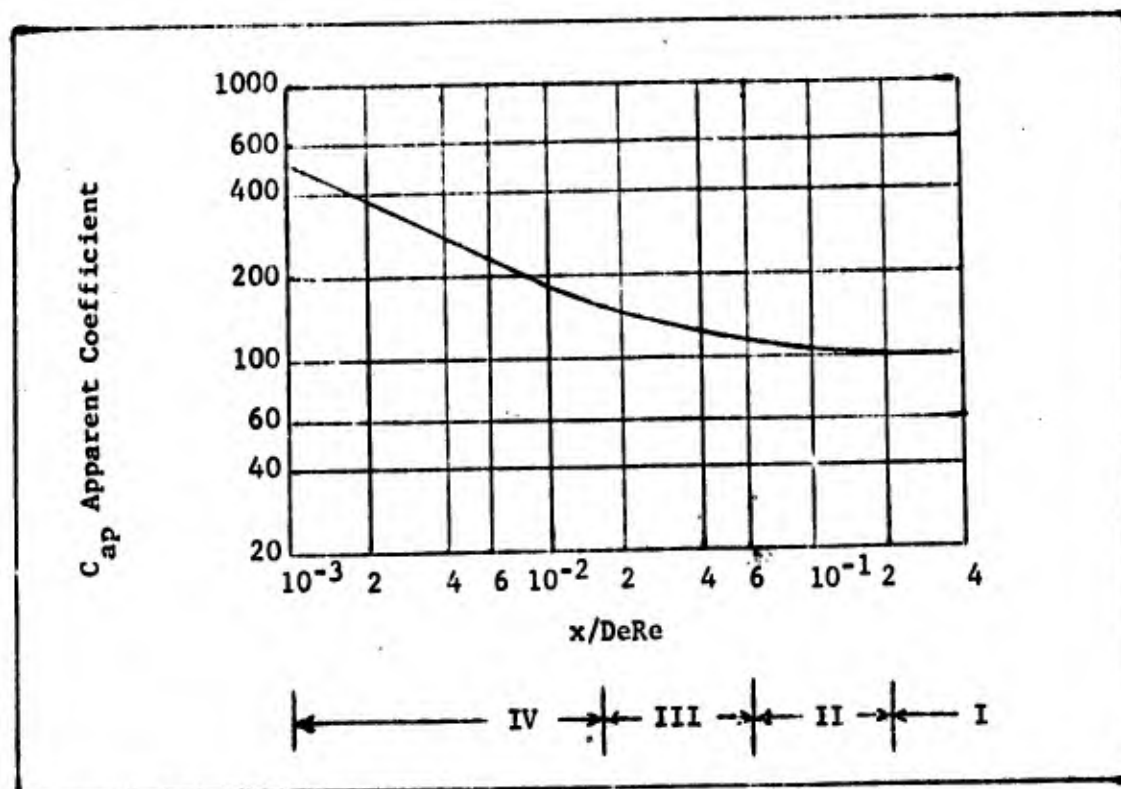
$$D = \frac{4lF_D}{3} \quad (49)$$

Substituting Eq's (48) into Eq (51), the generalized viscous damping force for the three different viscous oils can be written as

$$D = C_{ap}(0.2419 \times 10^{-3})\dot{\theta}(t) \frac{\text{Kgm}^2}{\text{sec}^2}, \text{ For 500 centistokes} \quad (50a)$$

$$D = C_{ap}(0.569 \times 10^{-3})\dot{\theta}(t) \frac{\text{Kgm}^2}{\text{sec}^2}, \text{ For 1000 centistokes} \quad (50b)$$

$$D = C_{ap}(0.9677 \times 10^{-3})\dot{\theta}(t) \frac{\text{Kgm}^2}{\text{sec}^2}, \text{ For 2000 centistokes} \quad (50c)$$

Fig. 12. Apparent Coefficient C_{ap}

To develop a general equation for C_{ap} , the curve shown in Fig. 12 was broken up into four linear regions (i.e. four straight lines).

By defining

$$\tau = \frac{x}{DeRe} \quad (51)$$

two arbitrary points (C_{ap1}, τ_1) and (C_{ap2}, τ_2) can be assigned to each straight line. The negative slope of each region can be determined from

$$s = \frac{\text{Log } C_{ap2} - \text{Log } C_{ap1}}{\text{Log } \tau_1 - \text{Log } \tau_2} \quad (52)$$

Knowing the slope and one point on the line, an equation for each straight line can be developed from

$$\text{Log } C_{ap} - \text{Log } C_{ap1} = -s(\text{Log } \tau - \text{Log } \tau_1) \quad (53)$$

Using the fundamental laws of logarithms the general equation for C_{ap} can be written as

$$C_{ap} = \frac{C_{ap1} \tau_1^s}{\tau^s} \quad (54)$$

Substituting Eq (51) into Eq (54) and using the general form of Eq's (33) (i.e. the Reynolds number can be written as $R_e = K_{Re} |\dot{\theta}(t)|$) yields

$$C_{ap} = C_{ap1} \tau_1^s \left(\frac{D_e K_{Re}}{x} \right)^s |\dot{\theta}(t)|^s \quad (55)$$

Table I

C_{ap} , τ , and s Matrix

| Region | C_{ap1} | C_{ap2} | τ_1 | τ_2 | s |
|--------|-----------|-----------|-----------|----------|---------|
| I | 100 | 100 | 10^{-3} | .4 | 0 |
| II | 165 | 100 | 10^{-3} | .2 | 0.09451 |
| III | 280 | 115 | 10^{-3} | .06 | 0.21734 |
| IV | 520 | 150 | 10^{-3} | .012 | 0.5003 |

Using Eq (30), Eq's (33), $x = 0.003m$, Table I, Eq (55) and Eq's (50) the generalized damping force can be shown to be of the form

$$D = D_{ij} = d_{ij} |\dot{\theta}(t)|^s j \ddot{\theta}(t) \frac{Kgm^2}{sec^2} \quad (56)$$

where $i = 1, 2, 3$, refers to the three kinematic viscosities given in Eq's (32) and $j = I, II, III, IV$, refers to the operating regions shown in Fig. 12. The real, positive constants, s_j and d_{ij} are tabulated in Table II.

Table II
Generalized Damping, d_{ij} , Matrix

| Region j $v_i \backslash s_j$ | I $\tau > .2$ | II .06 $\leq \tau \leq .2$ | III .012 $\leq \tau \leq .06$ | IV $\tau < .012$ |
|----------------------------------|-------------------------|-------------------------------|----------------------------------|--------------------------|
| | 0 | 0.0945 | 0.2173 | 0.5003 |
| $v_1 = 500$ c.s. | 0.2419×10^{-1} | 0.19376×10^{-1} | 0.14877×10^{-1} | 0.38341×10^{-2} |
| $v_2 = 1000$ c.s. | 0.5069×10^{-1} | 0.40299×10^{-1} | 0.26546×10^{-1} | 0.55606×10^{-2} |
| $v_3 = 2000$ c.s. | 0.9677×10^{-1} | 0.72132×10^{-1} | 0.34585×10^{-1} | 0.74929×10^{-2} |

In region I the generalized force, D_{iI} , may be considered a linear function of $\dot{\theta}(t)$ and can be represented by

$$D_{iI} = \beta l_0 \dot{\theta}(t) \frac{\text{Kgm}^2}{\text{sec}^2} \quad (57)$$

where β is a damping constant and l_0 is any reference length, included only to emphasize that D_{iI} is a moment. In Regions II, III, and IV the damping moment, D_{ij} is a non-linear function of $\dot{\theta}(t)$ as represented by Eq (56) and Table II.

Equation of Motion. The problem can now be formulated using Lagrange's equations, Eq's (1), and the generalized force equation, Eq (3). Let the generalized coordinates be $q_1 = X(t)$ and $q_2 = \theta(t)$. Then the generalized velocities are $\dot{q}_1 = \dot{X}(t)$ and $\dot{q}_2 = \dot{\theta}(t)$. From Eq (3), the generalized force, Q_1 , associated with the $X(t)$ coordinate is

$$Q_1 = F \quad (58)$$

because the potential energy and the generalized damping force are independent of coordinate $X(t)$. The generalized force, Q_2 , associated with the $\theta(t)$ coordinate is

$$Q_2 = - \frac{\partial V(\theta)}{\partial \theta} - D_{ij} \quad (59)$$

because the applied force is independent of the coordinate $\theta(t)$. Substituting Eq (21) into Eq (59) yields

$$Q_2 = - \frac{\partial}{\partial \theta} \left\{ mg\ell [1 - \cos\theta(t)] \right\} - D_{1j} \quad (60)$$

Substituting Eq's (17) and (58) into Lagrange's equations. Eq's (1), with $i = 1$ (i.e. with the generalized coordinate $X(t)$), the following equation can be written

$$\begin{aligned} \frac{d}{dt} \left\{ \frac{\partial}{\partial \dot{X}(t)} \left[\frac{1}{2} m\dot{X}(t)^2 - m\dot{X}(t)\ell\dot{\theta}(t) + \frac{2}{3} m\ell^2\dot{\theta}(t)^2 \right. \right. \\ \left. \left. + \frac{1}{2} M\dot{X}(t)^2 \right] \right\} - \frac{\partial}{\partial X(t)} \left[\frac{1}{2} m\dot{X}(t)^2 - m\dot{X}(t)\ell\dot{\theta}(t) \right. \\ \left. + \frac{2}{3} m\ell^2\dot{\theta}(t)^2 + \frac{1}{2} M\dot{X}(t)^2 \right] = F \end{aligned} \quad (61)$$

Performing the partial differentiation yields

$$\frac{d}{dt} \left[m\dot{X}(t) - m\ell\dot{\theta}(t) + M\dot{X}(t) \right] = F \quad (62)$$

Performing the differentiation and collecting like terms yields

$$(M-m)\ddot{X}(t) - m\ell\ddot{\theta}(t) = F \quad (63)$$

Substituting Eq's (17) and (60) into Lagrange's equations, Eq's (2), with $i = 2$ (i.e. with the generalized coordinate $\theta(t)$), the following equation can be written

$$\begin{aligned} \frac{d}{dt} \left\{ \frac{\partial}{\partial \dot{\theta}(t)} \left[\frac{1}{2} m\dot{X}(t)^2 - m\dot{X}(t)\ell\dot{\theta}(t) + \frac{2}{3} m\ell^2\dot{\theta}(t)^2 \right. \right. \\ \left. \left. + \frac{1}{2} M\dot{X}(t)^2 \right] \right\} - \frac{\partial}{\partial \theta(t)} \left[\frac{1}{2} m\dot{X}(t)^2 - m\dot{X}(t)\ell\dot{\theta}(t) \right. \\ \left. + \frac{2}{3} m\ell^2\dot{\theta}(t)^2 + \frac{1}{2} M\dot{X}(t)^2 \right] = - \frac{\partial}{\partial \theta} \left\{ mg\ell [1 - \cos\theta(t)] \right\} - D_{1j} \end{aligned} \quad (64)$$

Performing the partial differentiation yields

$$\frac{d}{dt} \left[-m\dot{X}(t) + \frac{4}{3} m^2 \dot{\theta}(t) \right] = -mg^l \sin\theta(t) - D_{ij} \quad (65)$$

Performing the differentiation and rearranging terms yields

$$\frac{4}{3} m^2 \ddot{\theta}(t) + D_{ij} + mg^l \sin\theta(t) = m\ddot{X}(t) \quad (66)$$

Concern here is only for the response of the pendulum to a given gage motion, so Eq (66) need be the only equation considered. Dividing both sides of Eq (66) by $4m^2/3$ yields

$$\ddot{\theta}(t) + \frac{3D_{ij}}{4m^2} + \frac{3g}{4l} \sin\theta(t) = \frac{3}{4l} X(t) \quad (67)$$

where

$$g = 9.8066 \frac{m}{\text{sec}^2} \quad m = 0.368 \times 10^{-1} \text{ Kg}$$

$$l = 0.205 \times 10^{-1} m$$

Substituting the values for g , l , and m into Eq (68) yields

$$\ddot{\theta}(t) + 48,496 D_{ij} + 358.78 \sin\theta(t) = 36.585 \ddot{X}(t) \quad (68)$$

Substituting D_{ij} from Eq (56) into Eq (68) the mechanical equation of motion can be written as

$$\ddot{\theta}(t) + K_{ij} |\dot{\theta}(t)|^s \dot{\theta}(t) + 358.78 \sin\theta(t) = 36.585 \ddot{X}(t) \quad (69)$$

where

$$K_{ij} = 48,496 d_{ij}$$

The value's for K_{ij} are tabulated in the section titled Overall System State Model.

Electrical Model

The two coils, E core, armature, and two resistors composing the electrical and magnetic circuit, are shown in Fig. 13. For the indicated winding sense and current direction the flux directions were found by applying the right hand rule to each coil (with the fingers wrapped around the coil in the direction of the natural current, the thumb will point in the direction of the flux).

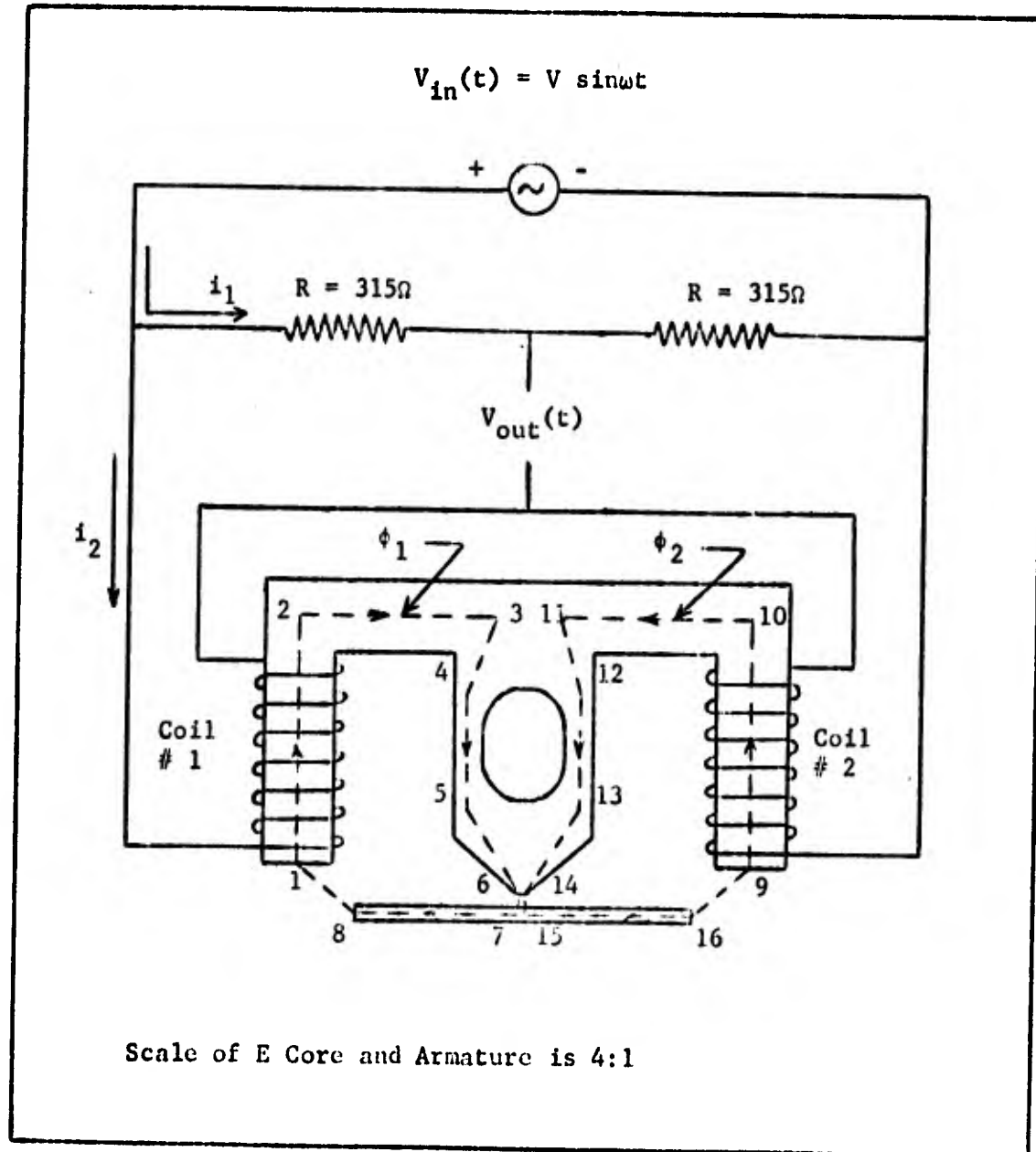


Fig. 13. The Electrical and Magnetic Circuit

Ampere's time-varying circuital law is

$$\oint \mathbf{H} \cdot d\mathbf{l} = \int_s (\nabla \times \mathbf{H}) \cdot d\mathbf{s} = \int_s \mathbf{J} \cdot d\mathbf{s} + \int_s \frac{\partial \mathbf{D}}{\partial t} \cdot d\mathbf{s} \quad (70)$$

where

\mathbf{H} = Magnetic field intensity

\mathbf{D} = Electric flux density

\mathbf{J} = Current density

The frequency of the current is low enough so that electromagnetic radiation is negligible. Then Ampere's time-varying circuital law can be approximated by

$$\oint \mathbf{H} \cdot d\mathbf{l} = \int_s (\nabla \times \mathbf{H}) \cdot d\mathbf{s} = \int_s \mathbf{J} \cdot d\mathbf{s} = \int_s \mathbf{J} \cdot \mathbf{n} ds \quad (71)$$

This law states that the line integral of the magnetic intensity \mathbf{H} around a closed contour is equal to the current across a surface bounded by the contour. The direction of the contour and the reference direction of the current across the surface bounded by the contour are related by the right-hand rule.

Ampere's circuital law Eq (71) can now be applied to the closed flux line ϕ_1 , shown dotted in Fig. 13. The current across the surface bounded by the contour is $N_1 i_2$, where N_1 is the number of turns of coil number one. Then

$$\oint \mathbf{H} \cdot d\mathbf{l} = N_1 i_2 \quad (72)$$

where

$$\mathbf{H} = a_x H_x + a_y H_y + a_z H_z$$

$$d\mathbf{l} = a_x d_x + a_y d_y + a_z d_z$$

Since the vectors \mathbf{H} and $d\mathbf{l}$ have the same direction at all the points

along the flux line, Eq (72), reduces to

$$\oint H dl = N_1 i_2 \quad (73)$$

The left-hand side of Eq (73) can now be expanded if the geometry of the core is taken into account and some approximations are made:

1. neglect the leakage flux.
2. assume that the total flux through any cross section is the same.
3. neglect the spreading of the flux at the corners.
4. assume that the cross section of the core at any point along one particular segment of the contour is one and the same.
5. assume that the flux is uniformly distributed at the various cross sections.

Then the flux ϕ_1 , through the core is

$$\begin{aligned} \phi_1 &= B_{12}A_{12} = B_{23}A_{23} = B_{34}A_{34} = B_{45}A_{45} = B_{56}A_{56} \\ &= B_{67}A_{67} = B_{78}A_{78} = B_{81}A_{81} \end{aligned} \quad (74)$$

where B_{12} is uniformly distributed flux density over an area A_{12} , which is the area of cross section at any point along the segment of the contour 1-2 etc. Exceptions are A_{34} , A_{56} , and A_{67} , which are one-half the area of cross section at any point along their segment.

The magnetic flux density and the magnetic field intensity are functionally related. The relationship between them is given by

$$B = \mu H \quad (75)$$

where μ is the permeability of the medium. The magnetic intensity along the individual segments can be written as

$$H_{12} = \frac{B_{12}}{\mu_{12}} \quad H_{23} = \frac{B_{23}}{\mu_{23}} \quad H_{34} = \frac{B_{34}}{\mu_{34}} \quad H_{45} = \frac{B_{45}}{\mu_{45}} \quad (76)$$

$$H_{56} = \frac{B_{56}}{\mu_{56}} \quad H_{67} = \frac{B_{67}}{\mu_{67}} \quad H_{78} = \frac{B_{78}}{\mu_{78}} \quad H_{81} = \frac{B_{81}}{\mu_{81}}$$

This enables the left-hand side of Eq (73) to be expanded.

$$\int_{12} H_{12} d\ell + \int_{23} H_{23} d\ell + \int_{34} H_{34} d\ell + \int_{45} H_{45} d\ell \quad (77)$$

$$\int_{56} H_{56} d\ell + \int_{67} H_{67} d\ell + \int_{78} H_{78} d\ell + \int_{81} H_{81} d\ell = N_{12}$$

or

$$H_{12}^{\ell}{}_{12} + H_{23}^{\ell}{}_{23} + H_{34}^{\ell}{}_{34} + H_{45}^{\ell}{}_{45} + H_{56}^{\ell}{}_{56} \quad (78)$$

$$H_{67}^{\ell}{}_{67} + H_{78}^{\ell}{}_{78} + H_{81}^{\ell}{}_{81} = N_{12}$$

Substituting Eq (76) into Eq (78) yields

$$\frac{B_{12}}{\mu_{12}} \ell_{12} + \frac{B_{23}}{\mu_{23}} \ell_{23} + \frac{B_{34}}{\mu_{34}} \ell_{34} + \frac{B_{45}}{\mu_{45}} \ell_{45} \quad (79)$$

$$\frac{B_{56}}{\mu_{56}} \ell_{56} + \frac{B_{67}}{\mu_{67}} \ell_{67} + \frac{B_{78}}{\mu_{78}} \ell_{78} + \frac{B_{81}}{\mu_{81}} \ell_{81} = N_{12}$$

Substituting for B yields

$$\frac{\phi_1 \ell_{12}}{A_{12}^{\mu}{}_{12}} + \frac{\phi_1 \ell_{23}}{A_{23}^{\mu}{}_{23}} + \frac{\phi_1 \ell_{34}}{A_{34}^{\mu}{}_{34}} + \frac{\phi_1 \ell_{45}}{A_{45}^{\mu}{}_{45}} \quad (80)$$

$$\frac{\phi_1 \ell_{56}}{A_{56}^{\mu}{}_{56}} + \frac{\phi_1 \ell_{67}}{A_{67}^{\mu}{}_{67}} + \frac{\phi_1 \ell_{78}}{A_{78}^{\mu}{}_{78}} + \frac{\phi_1 \ell_{81}}{A_{81}^{\mu}{}_{81}} = N_{12}$$

Solving for ϕ_1 , yields

$$\phi_1 = \frac{N_1 i_1}{R} \quad (81)$$

Where R is the total reluctance of the magnetic circuit and

$$R = \frac{l_{12}}{A_{12} \mu_{12}} + \frac{l_{23}}{A_{23} \mu_{23}} + \frac{l_{34}}{A_{34} \mu_{34}} + \frac{l_{45}}{A_{45} \mu_{45}} \quad (82)$$

$$+ \frac{l_{56}}{A_{56} \mu_{56}} + \frac{l_{67}}{A_{67} \mu_{67}} + \frac{l_{78}}{A_{78} \mu_{78}} + \frac{l_{81}}{A_{81} \mu_{81}}$$

The permeability of a medium can be expressed in terms of that of free space. Thus

$$\mu = \mu_r \mu_0 \quad (83)$$

where $\mu_0 = 4 \times 10^{-7}$ henry per meter is the permeability of free space, and μ_r is the relative permeability which depends on the medium. The material composing the E core and armature is "45 Permalloy." (Note: this information was obtained in a telephone call with Bob Bunker, Asst. Chief Experimental Branch of the Civil Engineering Research Division, Air Force Weapons Laboratory, Kirtland Air Force Base, New Mexico, on 29 December, 1972. The approximate composition of "45 Permalloy" is 45% Ni and 55% Fe). The relative permeability of this material is approximately 2,500 (13). The relative permeability of the oil can be considered approximately one (i.e. the permeability of the oil is essentially the permeability of free space μ_0). Then the permeability of the different segments of the core and armature are

$$\mu_{12} = \mu_{23} = \mu_{34} = \mu_{45} = \mu_{56} = \mu_{78} = 2,500 \mu_0 \quad (84)$$

Similarly the permeability of the oil gaps are

$$\mu_{67} = \mu_{81} = \mu_0 \quad (85)$$

Then the total reluctance of the magnetic circuit can be written as

$$R = \frac{l_{12}}{A_{12} 2,500 \mu_0} + \frac{l_{23}}{A_{23} 2,500 \mu_0} + \frac{l_{34}}{A_{34} 2,500 \mu_0} + \frac{l_{45}}{A_{45} 2,500 \mu_0} \quad (86)$$

$$+ \frac{l_{56}}{A_{56} 2,500 \mu_0} + \frac{l_{67}}{A_{67} \mu_0} + \frac{l_{78}}{A_{78} 2,500 \mu_0} + \frac{l_{81}}{A_{81} \mu_0}$$

Thus the reluctance of the core is very small compared to that of the oil gaps. Then Eq (81) can be approximated by

$$\phi_1 = \frac{N_1 i_2}{\frac{l_{81}}{A_{81} \mu_0} + \frac{l_{67}}{A_{67} \mu_0}} \quad (87)$$

Again applying Ampere's circuital law, Eq (71) to the contour 1-2-10-9-16-8-1 (Ref. Fig. 13), it can be determined if a mutual flux, ϕ_{m1} , exists. The current that passes across the surface bounded by this contour is $N_1 i_2 - N_2 i_2$, where N_1 is the number of turns in coil number two. The number of turns in coil number one is equal to the number of turns in coil number two, thus

$$\oint H \cdot d\ell = 0 \quad (88)$$

Hence it can be concluded that the mutual flux, ϕ_{m1} , is zero.

Applying Ampere's circuital law, Eq (71) to the closed flux line ϕ_2 , shown dotted in Fig. 13, an expression similar to Eq (87) can be worked out for ϕ_2 .

$$\phi_2 = \frac{N_2 i_2}{\frac{l_{916}}{A_{916} \mu_0} + \frac{l_{1415}}{A_{1415} \mu_0}} \quad (89)$$

Similarly a mutual flux, ϕ_{m2} , can be shown to be zero, by applying Ampere's to the contour 9-10-2-1-8-16-9.

Inductance Equations. The inductance of coil number one is equal to its flux linkage per ampere:

$$L_1 = \frac{\lambda_1}{i_1} \quad (90)$$

The flux linkage, λ , is defined as the flux through the core times the number of turns of the coil. Then Eq (90) can be written as

$$L_1 = \frac{N_1 \phi_1}{i_1} \quad (91)$$

Substituting Eq (87) into (91) yields

$$L_1 = \frac{N_1^2}{\frac{l_{81}}{A_{81} \mu_o} + \frac{l_{67}}{A_{67} \mu_o}} \quad (92)$$

Similarly the inductance of coil number two is

$$L_2 = \frac{N_2 \phi_2}{i_2} \quad (93)$$

Substituting Eq (89) into Eq (93) yields

$$L_2 = \frac{N_2^2}{\frac{l_{916}}{A_{916} \mu_o} + \frac{l_{1415}}{A_{1415} \mu_o}} \quad (94)$$

The distances of the oil gap l_{81} and l_{916} change when the pendulum rotates. If the distance l_{81} increases the reluctance of the magnetic circuit for coil number one will increase and consequently the inductance,

L_1 , will decrease. At the same time $l_{9\ 16}$ will have decreased by the same amount that l_{81} increased. Consequently the inductance, L_2 , will have increased by the same amount L_1 has decreased. Since l_{81} and $l_{9\ 16}$ are functions of time, L_1 and L_2 will also be functions of time.

The distances $l_{81}(t)$ and $l_{9\ 16}(t)$ can be written in terms of $\theta(t)$. Referring to Fig. 14, it can be seen that by applying the law of cosines:

$$l_{81}(t) = \sqrt{d_3^2 + d_2^2 - 2d_3d_2\cos(\theta(t) + \beta)} \quad (95)$$

where

$$d_3 = \sqrt{d_1^2 + c^2}$$

$$\beta = \left(\tan^{-1} \frac{c}{d_1} \right) \left(\frac{\pi}{180^\circ} \right)$$

Substituting Eq (95) into Eq (92) yields

$$L_1(t) = \frac{N_1^2}{\frac{\sqrt{d_3^2 + d_2^2 - 2d_3d_2\cos(\theta(t) + \beta)}}{A_{81}\mu_0} + \frac{l_{67}}{A_{67}\mu_0}} \quad (96)$$

Similarly referring to Fig. 15 it can be seen that by applying the law of cosines:

$$l_{9\ 16}(t) = \sqrt{d_3^2 + d_2^2 - 2d_3d_2\cos(\theta(t) - \beta)} \quad (97)$$

where

$$d_3 = \sqrt{d_1^2 + c^2}$$

$$\beta = \left(\tan^{-1} \frac{c}{d_1} \right) \left(\frac{\pi}{180^\circ} \right)$$

Substituting Eq (97) into Eq (94) yields

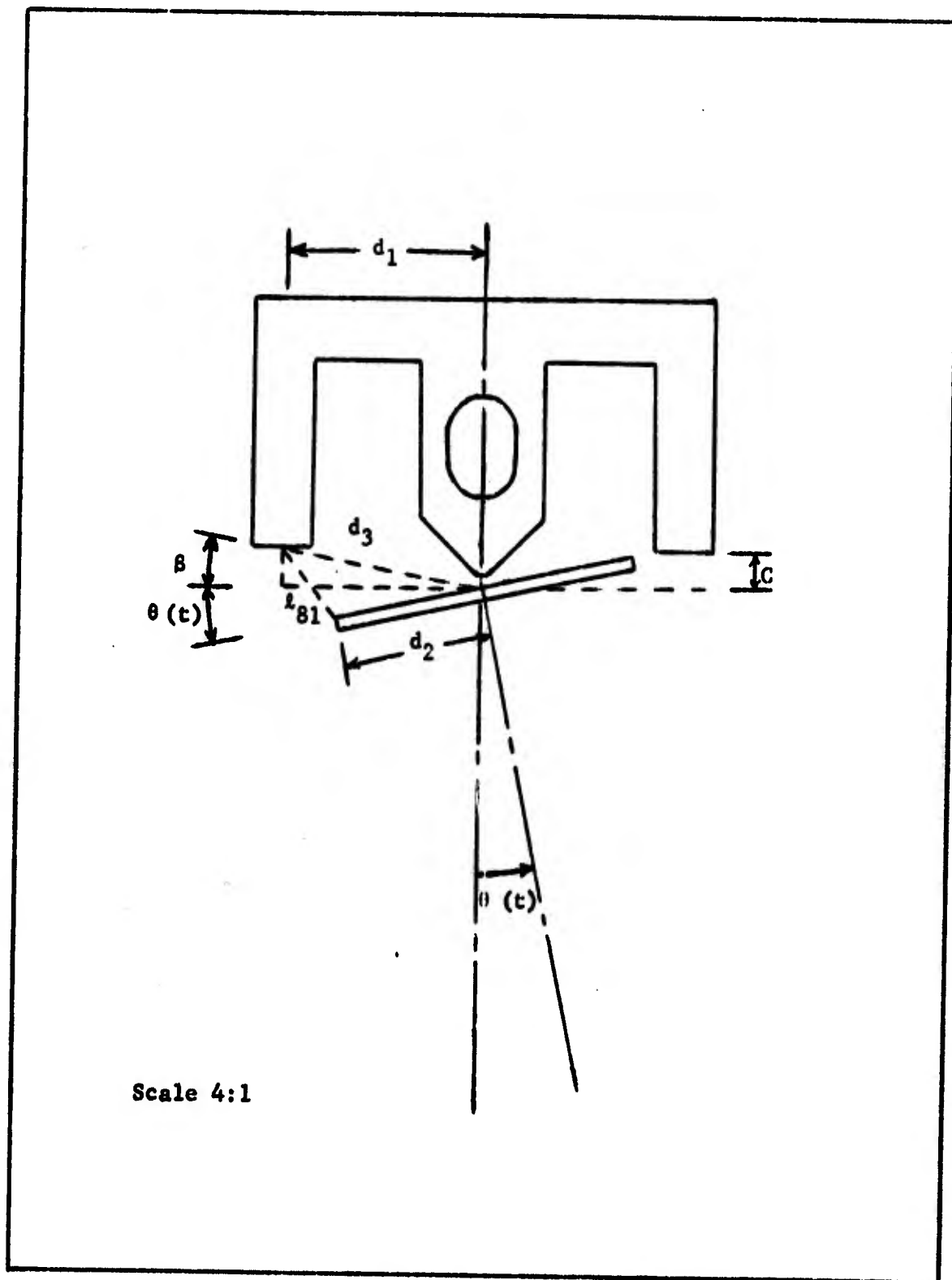


Fig. 14. Oil Gap Distance l_{g1} , with $\theta(t) = 12^\circ$

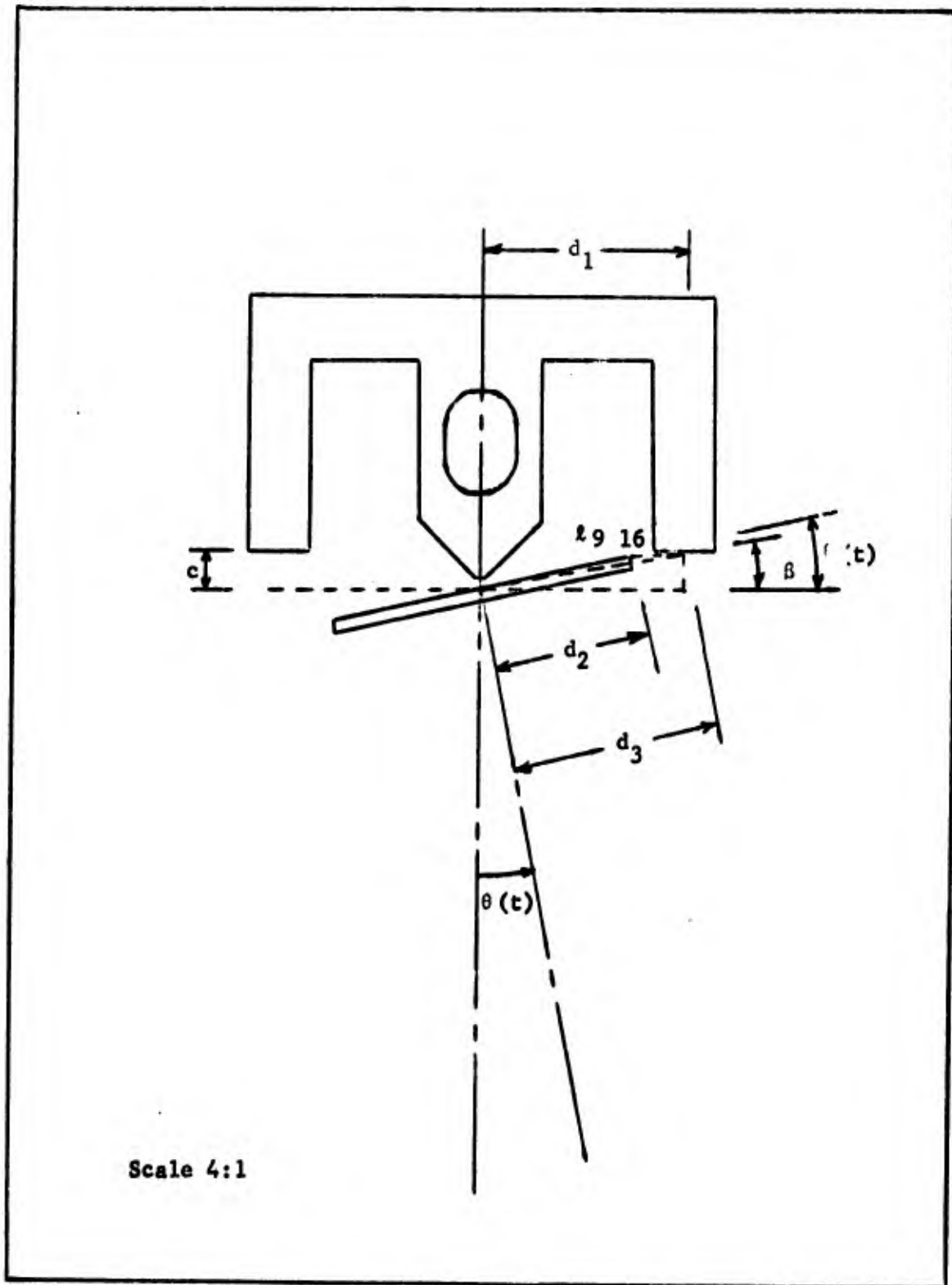


Fig. 15. Oil Gap Distance 9.16, with $\theta(t) = 12^\circ$

$$L_2(t) = \frac{N_2^2}{\frac{\sqrt{d_3^2 + d_2^2 - 2d_3d_2\cos(\theta(t) - \epsilon)}}{A_9 16^{\mu_0}} + \frac{l_{14} 15}{A_{14} \cdot 15^{\mu_0}}} \quad (98)$$

Electrical System Equations.

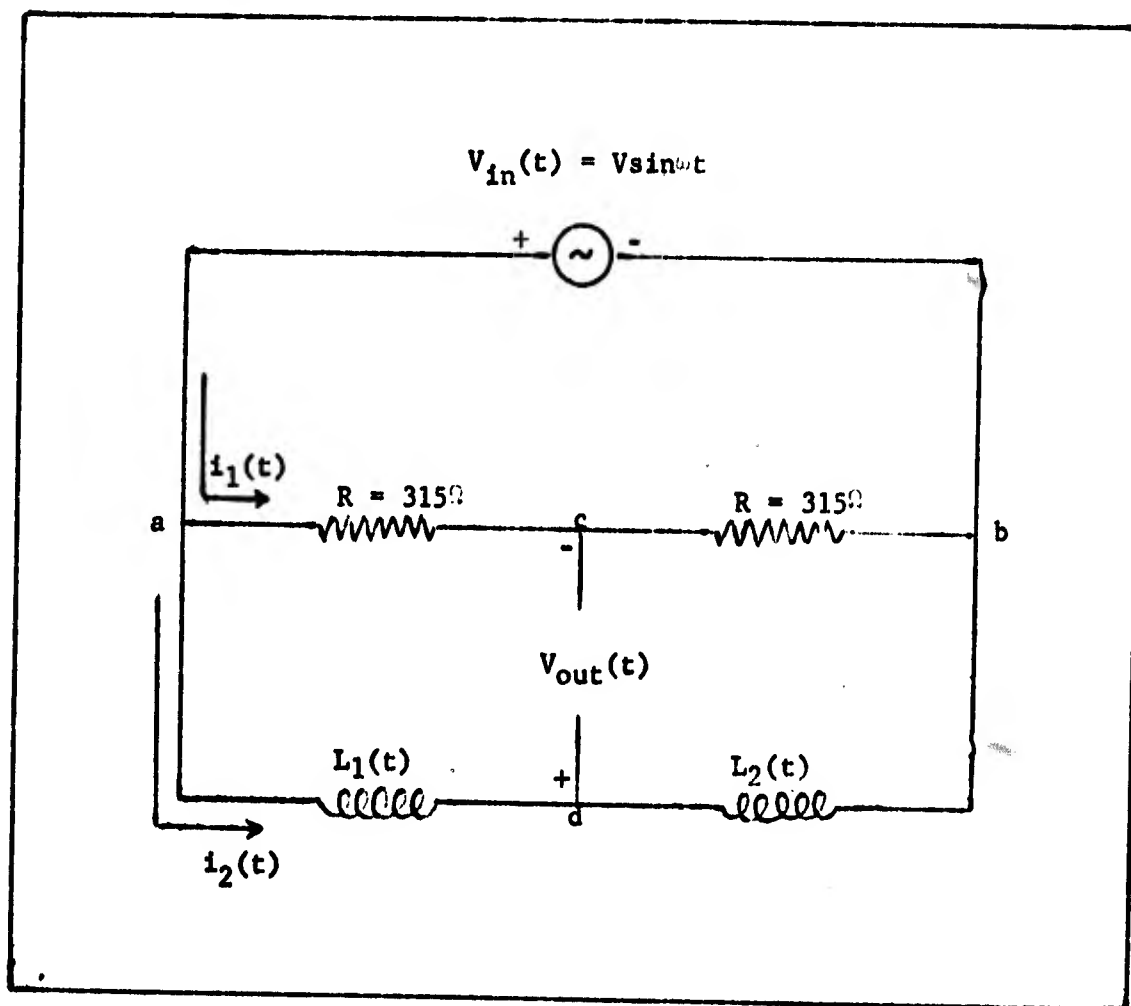


Fig. 16. Equivalent Circuit

The equivalent circuit shown in Fig. 16 is a standard AC-bridge circuit. The condition of balance is the condition of zero difference of potential from c to d. This requires that the voltage drop from a to c equal the voltage drop from a to d, or

$$i_1(t)R = i_2(t)L_1(t) \quad (99)$$

and similarly

$$i_1(t)R = i_2(t)L_2(t) \quad (100)$$

Since the two resistors have the same value this condition only occurs when $L_1(t) = L_2(t)$. In the balance condition $v_{in}(t)/2$ will appear across each element of the bridge. If L_1 decreases, a voltage less than $v_{in}(t)/2$ will appear across the terminals a to d. Then L_2 will have increased by the same amount L_1 has decreased, resulting in an increased voltage of the same magnitude across d to b as the voltage across a to d was decreased. The output of the bridge will be the difference in potential from c to d.

The state equation for the bridge circuit can now be developed. By assigning the current through the inductors as the state variable and applying Kirchhoff's voltage law to the bridge circuit the following equation can be written.

$$v_{in}(t) = \frac{d}{dt} [L_1(t)i_2(t)] + \frac{d}{dt} [L_2(t)i_2(t)] \quad (101)$$

Performing the differentiation and collecting like terms yields

$$v_{in}(t) = [L_1(t) + L_2(t)] \frac{di_2(t)}{dt} + \left[\frac{dL_1(t)}{dt} + \frac{dL_2(t)}{dt} \right] i_2(t) \quad (102)$$

Solving for $di_2(t)/dt$, the electrical state equation can be written as

$$\frac{di_2(t)}{dt} = - \left[\frac{1}{L_1(t) + L_2(t)} \right] \left[\frac{dL_1(t)}{dt} + \frac{dL_2(t)}{dt} \right] i_2(t) + \left[\frac{1}{L_1(t) + L_2(t)} \right] v_{in}(t) \quad (103)$$

For time, $t < 0$, the pendulum is stationary, thus the inductances L_1 and L_2 are constants. The bridge circuit is in a steady state condition. Then Eq (103) reduces to

$$\frac{di_2(t)}{dt} = \left(\frac{1}{L_1 + L_2} \right) v_{in}(t) \quad (104)$$

where $v_{in}(t) = V \sin \omega t$

integrating with respect to time from $-\infty$ to some time less than zero yields

$$i_2(t) = - \left[\frac{V}{\omega(L_1 + L_2)} \right] \cos \omega t \quad (105)$$

The initial condition for the current, i_2 , is

$$i_2(0) = - \frac{V}{\omega(L_1 + L_2)} \quad (106)$$

Applying Kirchhoff's voltage law to the bridge circuit, the output equation can be written as

$$V_{out}(t) = i_1 R - \frac{d}{dt} [L_1(t) i_2(t)] \quad (107)$$

Performing the differentiation and rearranging terms yield

$$V_{out}(t) = - \frac{dL_1(t)}{dt} i_2(t) - L_1(t) \frac{di_2(t)}{dt} + i_1 R \quad (108)$$

Also applying Kirchhoff's voltage law to the bridge circuit yields

$$V_{in}(t) = 2i_1(t)R \quad (109)$$

thus

$$i_1(t)R = \frac{V_{in}(t)}{2} \quad (110)$$

Substituting Eq's (110) and (103) into Eq (108) and collecting like coefficients, the electrical output equation can be written as

$$V_{\text{out}}(t) = \left\{ -\frac{dL_1(t)}{dt} + L_1(t) \left[\frac{1}{L_1(t) + L_2(t)} \right] \left[\frac{dL_1(t)}{dt} + \frac{dL_2(t)}{dt} \right] \right\} i_2(t) + \left\{ -L_1(t) \left[\frac{1}{L_1(t) + L_2(t)} \right] + \frac{1}{2} \right\} v_{\text{in}}(t) \quad (111)$$

The electrical system equations can then be summarized. The state equation is

$$\frac{di_2(t)}{dt} = f_3 \left[L_1(t), L_2(t), \frac{dL_1(t)}{dt}, \frac{dL_2(t)}{dt}, i_2(t), v_{\text{in}}(t) \right] \quad (112)$$

where F_3 is given by Eq (103). The initial condition $i_2(0)$ is given by Eq (106). The output equation is

$$V_{\text{out}}(t) = g_1 \left[L_1(t), L_2(t), \frac{dL_1(t)}{dt}, \frac{dL_2(t)}{dt}, i_2(t), v_{\text{in}}(t) \right] \quad (113)$$

where g_1 is given by Eq (111). The inductance equations used in the system equations are

$$L_1(t) = h_1 [\theta(t)] \quad (114)$$

where h_1 is given by Eq (96),

$$\frac{dL_1(t)}{dt} = h_2 [\theta(t), \dot{\theta}(t)] \quad (115)$$

where

$$h_2 = \frac{(-N_1^2 A_{81} A_{67} \mu_0) \left[\frac{2A_{81}^2 d_3 d_2 \dot{\theta} \sin(\theta(t) + \beta)}{2A_{67} \sqrt{d_3^2 + d_2^2 - 2d_3 d_2 \cos(\theta(t) + \beta)}} \right]}{\left[A_{67} \sqrt{d_3^2 + d_2^2 - 2d_3 d_2 \cos(\theta(t) + \beta)} + A_{81}^2 \mu_0 \right]^2} \quad (116)$$

and

$$L_2(t) = h_3 [\theta(t)] \quad (117)$$

where h_3 is given by Eq (98), and

$$\frac{dL_2(t)}{dt} = h_4 [\theta(t), \dot{\theta}(t)] \quad (118)$$

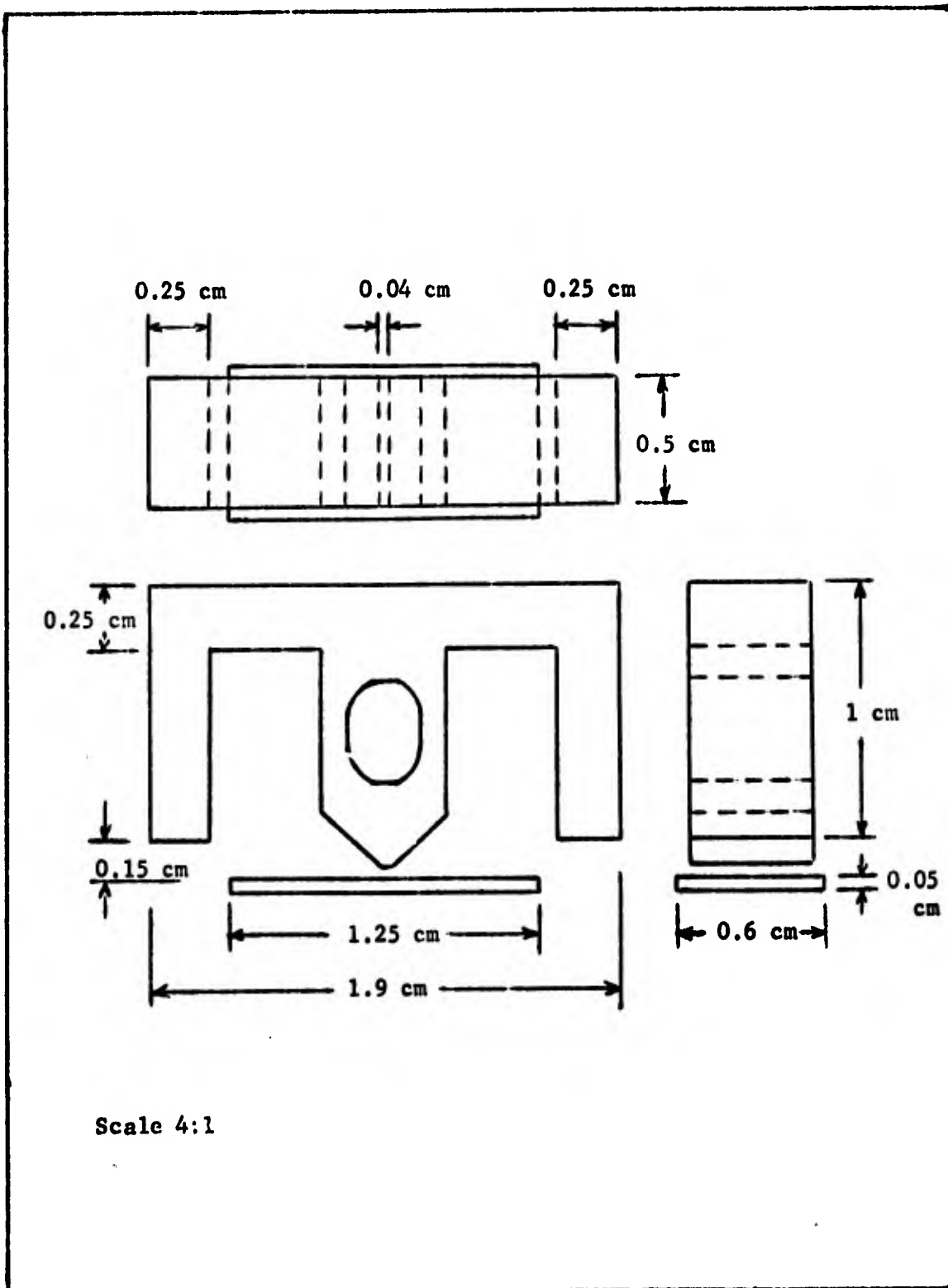


Fig. 17. E Core and Armature

where

$$h_4 = \frac{(-N_2^2 A_{916} A_{1415} \mu_o) \left[\frac{2A_{1415}^2 d_3 d_2 \sin(\theta(t) - \beta)}{2A_{1415} \sqrt{d_3^2 + d_2^2} - 2d_3 d_2 \cos(\theta(t) - \beta)} \right]}{\left[A_{1415} \sqrt{d_3^2 + d_2^2} - 2d_3 d_2 \cos(\theta(t) - \beta) + A_{916} \right]^2} \quad (119)$$

The constants used in the system equations are

$$v = 10\sqrt{2} \text{ volts} \quad (120a)$$

$$f = 3000 \text{ Hz} \quad (120b)$$

$$\omega = 2\pi f = 18,849.56 \text{ rad/sec} \quad (120c)$$

$$N_1 = N_2 = 550 \text{ turns} \quad (120d)$$

$$\mu_o = 4\pi \times 10^{-7} \text{ henry's per meter} \quad (120e)$$

and referring to Figs. 13 and 17, it can be concluded that

$$A_{81} = A_{916} = (0.5 \times 10^{-2} \text{ m})(0.25 \times 10^{-2} \text{ m}) = 0.125 \times 10^{-4} \text{ m}^2 \quad (120f)$$

$$A_{67} = A_{1415} = \frac{1}{2} (0.4 \times 10^{-3} \text{ m})(0.5 \times 10^{-3} \text{ m}) = 0.1 \times 10^{-5} \text{ m}^2 \quad (120g)$$

$$l_{67} = l_{1415} = 0.5 \times 10^{-3} \text{ m} \quad (120h)$$

referring to Figs. 14, 15, and 17

$$d_1 = 0.825 \times 10^{-2} \text{ m} \quad (120i)$$

$$d_2 = \frac{1}{2} (0.125 \times 10^{-1} \text{ m}) = 0.625 \times 10^{-2} \text{ m} \quad (120j)$$

$$c = 0.15 \times 10^{-2} \text{ m} \quad (120k)$$

$$d_3 = \sqrt{d_1^2 + c^2} = 0.83853 \times 10^{-2} \text{ m} \quad (120l)$$

$$\beta = \left(\tan^{-1} \frac{c}{d_1} \right) \left(\frac{\pi}{180^\circ} \right) = 0.17986 \text{ rads} \quad (120m)$$

Overall System State Model

The mechanical equation of motion is given by Eq (69). The electrical state equation is given by Eq (103). The electrical output equation is given by Eq (111). Defining the overall state variables as

$$x_1(t) = \theta(t) \quad (121a)$$

$$x_2(t) = \dot{\theta}(t) \quad (121b)$$

$$x_3(t) = i_2(t) \quad (121c)$$

The overall system equations can be written as

$$\dot{x}_1(t) = f_1 [x_2(t)] \quad (122a)$$

$$\dot{x}_2(t) = f_2 [x_1(t), x_2(t), \ddot{X}(t)] \quad (122b)$$

$$\dot{x}_3(t) = f_3 [x_1(t), x_2(t), x_3(t), v_{in}(t)] \quad (122c)$$

$$v_{out}(t) = g_1 [x_1(t), x_2(t), x_3(t), v_{in}(t)] \quad (122d)$$

The overall system equations are

$$\dot{x}_1(t) = x_2(t) \quad (123a)$$

$$\dot{x}_2(t) = -K_{ij} |x_2(t)|^{\beta} x_2(t) - 358.78 \sin x_1(t) + 36.585 \ddot{X}(t) \quad (123b)$$

$$\dot{x}_3(t) = \left[\frac{1}{L_1(t) + L_2(t)} \right] \left[\frac{dL_1(t)}{dt} + \frac{dL_2(t)}{dt} \right] x_3(t) + \left[\frac{1}{L_1(t) + L_2(t)} \right] v_{in}(t) \quad (123c)$$

$$v_{out}(t) = \left\{ -\frac{dL_1(t)}{dt} + L_1(t) \left[\frac{1}{L_1(t) + L_2(t)} \right] \left[\frac{dL_1(t)}{dt} + \frac{dL_2(t)}{dt} \right] \right\} x_3(t) \\ + \left\{ -L_1(t) \left[\frac{1}{L_1(t) + L_2(t)} \right] + \frac{1}{2} \right\} v_{in}(t) \quad (123d)$$

The initial condition $x_3(0)$ is

$$x_3(0) = -\frac{V}{\omega(L_1 + L_2)} \quad (124)$$

The inductance equations used in the overall system equations are

$$L_1(t) = h_1 [x_1(t)] \quad (125)$$

where

$$h_1 = \frac{N_1^2}{\sqrt{d_3 + d_2 - 2d_3d_2\cos(x_1(t) + \beta)}} + \frac{l_{67}}{A_{67}\mu_0} \quad (126)$$

$$\frac{dL_1(t)}{dt} = h_2 [x_1(t), x_2(t)] \tag{127}$$

where

$$h_2 = \frac{-N_1^2 A_{81} A_{67}^{\mu_0} \left[\frac{2A_{81}^2 d_3 d_2 x_2(t) \sin(x_1(t) + \beta)}{2A_{67} \sqrt{d_3^2 + d_2^2 - 2d_3 d_2 \cos(x_1(t) + \beta)}} \right]}{\left[A_{67} \sqrt{d_3^2 + d_2^2 - 2d_3 d_2 \cos(x_1(t) + \beta)} + A_{81}^2 A_{67} \right]^2} \tag{128}$$

$$L_2(t) = h_3 [x_1(t)] \tag{129}$$

where

$$h_3 = \frac{N_2^2}{\frac{\sqrt{d_3^2 + d_2^2 - 2d_3 d_2 \cos(x_1(t) - \beta)}}{A_9 16^{\mu_0}} + \frac{A_{14} 15}{A_{14} 15^{\mu_0}}} \tag{130}$$

$$\frac{dL_2(t)}{dt} = h_4 [x_1(t), x_2(t)] \tag{131}$$

where

$$h_4 = \frac{(-N_2^2 A_9 16 A_{14} 15^{\mu_0}) \left[\frac{2A_{14} 15^2 d_3 d_2 x_2(t) \sin(x_1(t) - \beta)}{2A_{14} 15 \sqrt{d_3^2 + d_2^2 - 2d_3 d_2 \cos(x_1(t) - \beta)}} \right]}{\left[A_{14} 15 \sqrt{d_3^2 + d_2^2 - 2d_3 d_2 \cos(x_1(t) - \beta)} + A_9 16^2 A_{14} 15 \right]^2} \tag{132}$$

Using Eq (69) and Table II, K_{ij} and s_j can be tabulated as shown in Table III.

Table III

K_{ij} Matrix

| Region j s _j | I $\tau > .2$ | II .06 ≤ τ ≤ .2 | III .012 ≤ τ < .06 | IV $\tau < .012$ |
|----------------------------|------------------|--------------------|-----------------------|---------------------|
| | v_1 | 0 | 0.0945 | 0.2173 |
| $v_1 = 500$ c.s. | 1173.1 | 939.66 | 721.48 | 185.94 |
| $v_2 = 1000$ c.s. | 2458.3 | 1954.3 | 1287.4 | 269.67 |
| $v_3 = 2000$ c.s. | 4693.0 | 3498.1 | 1677.2 | 363.38 |

III. Simulation

Description of the Computer Program

A computer program using a fourth-order, Runge-Kutta algorithm was developed to solve the overall system equations. Eq's (123a), (123b), (123c), and (123d) and the corresponding inductance Eq's (125), (127), (129), and (131). A programming listing is contained in Appendix B. The Runge-Kutta algorithm is well documented and, therefore it is not discussed, but the steps in the main program are listed with a few amplifying statements:

1. The constants, Eq's (120), used in the system equation are read in.
2. The time is set equal to zero.
3. The initial conditions $x_1(0)$ and $x_2(0)$ are read in. Then using Eq (124) and the corresponding inductance equations, Eq's (125) and (129, the initial condition $x_3(0)$ is calculated.
4. All initial conditions are then printed.
5. A loop for a time increment of approximately 21 microsec's is started. (Note - since the input voltage is a sine wave with a frequency of 3 KHz, using a time increment of approximately 21 microsec's, the wave is sampled 16 times each period).
6. The equations that generate the time dependent acceleration wave form are then calculated for the latest time.
7. Using the latest value of $x_1(t)$, the equation for τ , Eq (51), is calculated. The value of τ determines which state equation for $\dot{x}_2(t)$ to use.

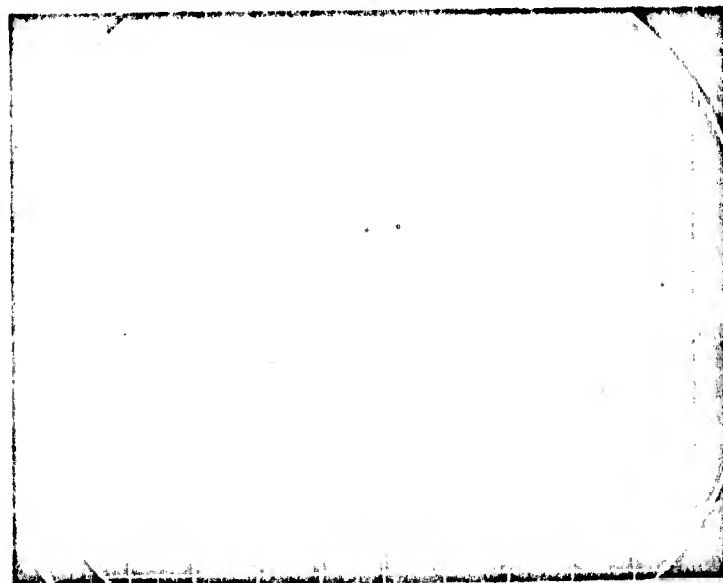
8. The overall system equations and the corresponding inductance equations are then calculated for the latest time.
9. Four passes at the Runge-Kutta subroutine are made updating the derivatives $x_1(t)$, $x_2(t)$ and $x_3(t)$ on each pass. On the last pass $t = t + \Delta t$.
10. The voltage output, Eq (123d), the voltage in, and the velocity, are calculated using the latest updated values.
11. The values for the state variables, voltage out, voltage in, velocity, τ , and time are printed for that time step.
12. If the time is less than the specified stopping time, the algorithm is started again by returning to the equations that generate the acceleration wave form in step 6.

In Appendix A, the symbols used in the main program are related to the symbols used in the model.

Verification of the Overall System State Model

A Sparton Model 601M horizontal velocity gage, filled with an oil of 1,000 centistokes, was obtained from the Weapons Laboratory, Kirtland AFB, New Mexico. Experimentation was done with the gage in the electrical engineering laboratory at the Air Force Institute of Technology. The two coils in the gage were electrically connected with two 315 ohm resistors to form a bridge. The input to the bridge was a 3 KHz, 10 volt RMS sine wave. The bridge output was monitored by a tektronix oscilloscope. The gage was then tilted to one side causing the pendulum to swing and hit its stop. When the gage was returned to its normal upright position the force of gravity acted on the pendulum causing it to rotate back to the equilibrium position, displacing oil as it went. A time-delayed picture of the bridge output

voltage as shown on the scope is shown in Fig. 18. The time and voltage scales on the oscilloscope picture are 2 sec./div. and 0.2 volts/div. respectively. This voltage wave form was plotted in Fig. 19 as shown by the solid line.



Reproduced from
best available copy.

Fig. 18. Oscilloscope Picture of Output Voltage

The computer program was used to verify the model against the experimental results. The initial conditions on the state variables from the laboratory set-up were

$$x_1(0) = 12^\circ \quad x_2(0) = 0 \quad x_3(0) = \frac{V}{\omega(L_1 + L_2)}$$

The forcing function was zero. The overall system equations for these initial conditions were solved. Superimposing the computer results, depicted by the broken line in Fig. 19, over the experimental results shows a nearly identical curve. A major source of the small error that does exist is due to the inaccuracy of reading points on the oscilloscope picture (Fig. 18).

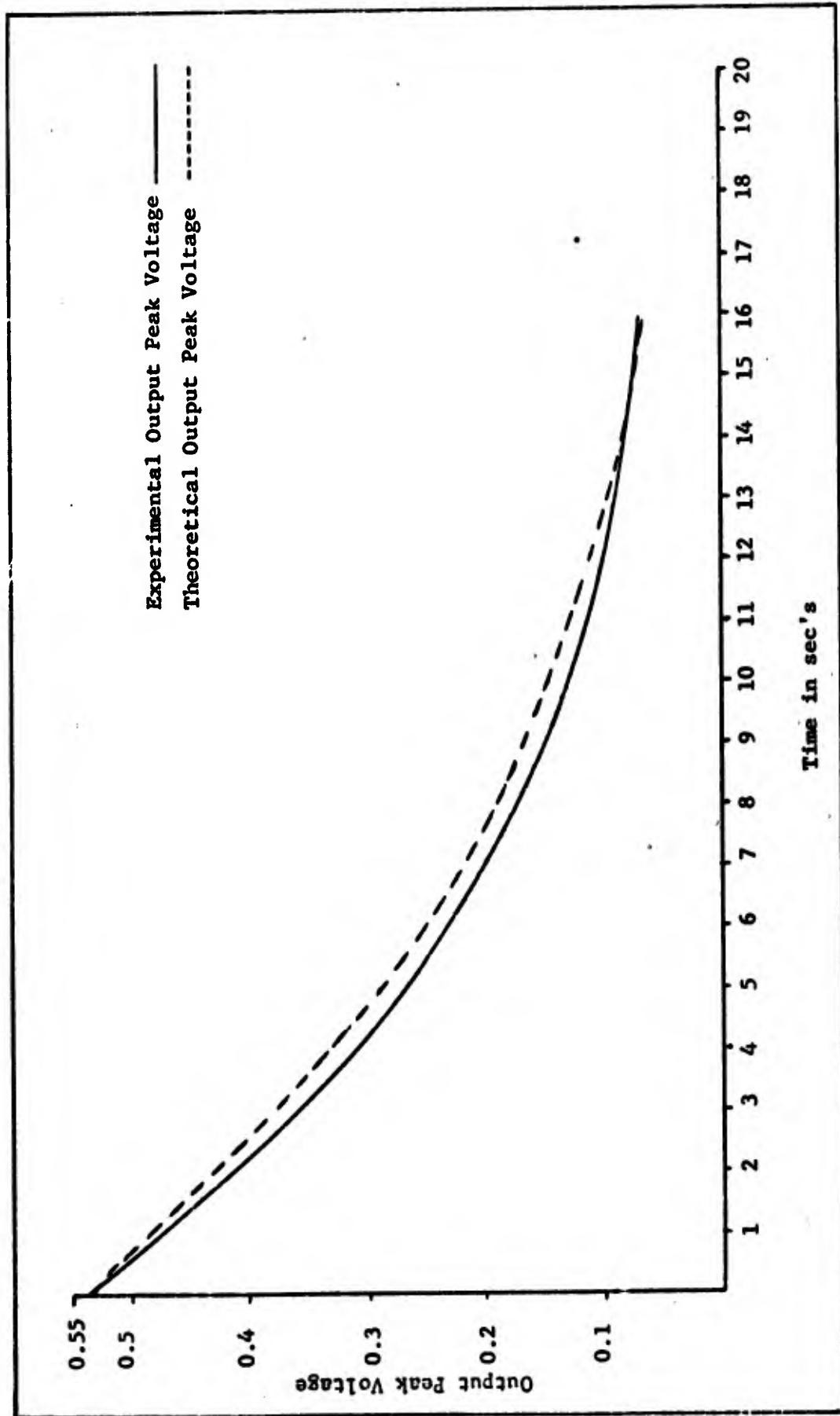


Fig. 19. Comparison of Experimental and Theoretical Output Peak Voltage for an Unforced System

Operating Range of the Gage

To determine the operating range of the gage for oil viscosities of 500, 1,000, and 2,000 centistokes a constant acceleration was applied to the gage. The time it took for θ to reach the maximum deflection of 12° (t_{\max}) was determined and is shown in Figures 20-25. The different regions of operation are also shown. Note that it is possible to obtain the velocity at any time from the product of the acceleration coordinate and time coordinate. Break-point accelerations, which divide the various operating regions after sufficient time, are shown in Table IV. A_{ij} and t_{ij} are defined from the curve, Fig. 20-25 such that A less than A_{ij} implies operation in region j for viscosity and $A = A_{ij} + \epsilon$, where ϵ is small, and t is greater than t_{ij} implies operation in region $(j + 1)$ for viscosity i .

Table IV

Break-Point Accelerations (A_{ij} in G's) and Times (t_{ij} in msec)

| Viscosity Region | $i = 1$ 500 c.s. | $i = 2$ 1000 c.s. | $i = 3$ 2000 c.s. |
|---------------------|---------------------|----------------------|----------------------|
| $j = I$ | 18.5 | 76.5 | 295 |
| | 7.1 | 5 | 1.4 |
| $j = II$ | 70 | 295 | 1100 |
| | 3.9 | 2.2 | 1.7 |

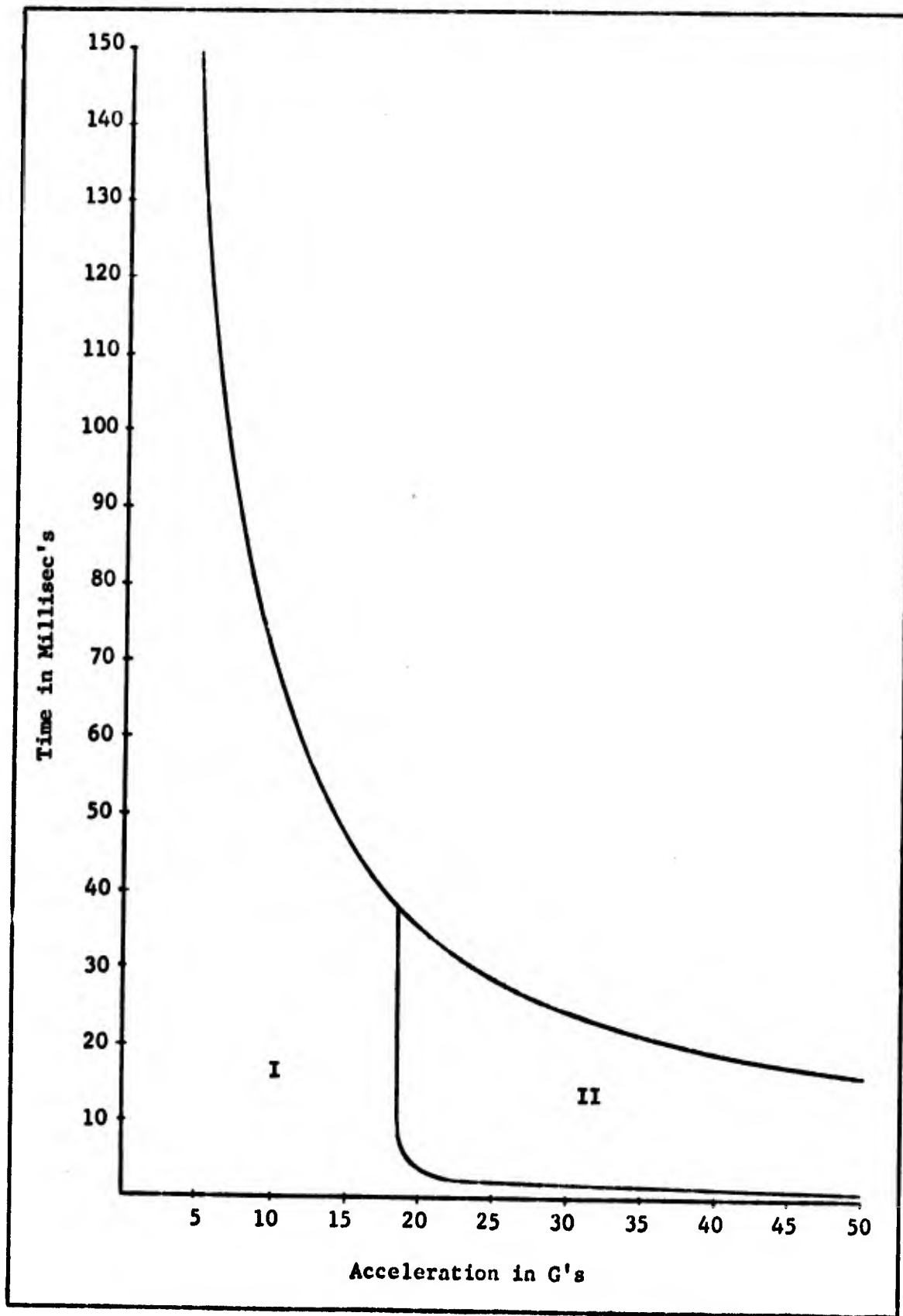


Fig. 20. Time for Maximum Deflection (t_{max}), $v_1 = 500$ c.s.
(Low Accelerations)

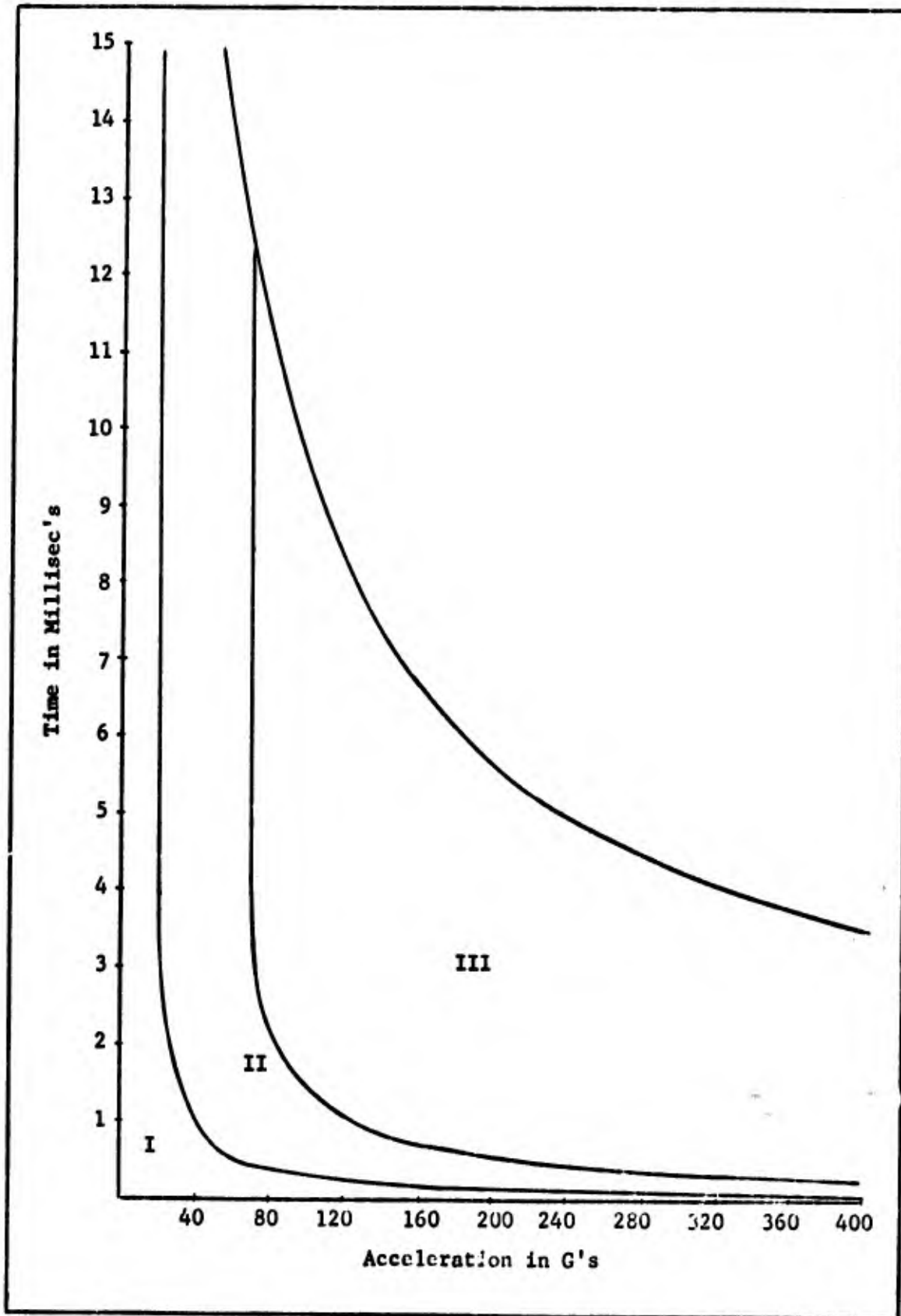


Fig. 21. Time for Maximum Deflection (t_{\max}), $v_1 = 500$ c.s.
(High Accelerations)

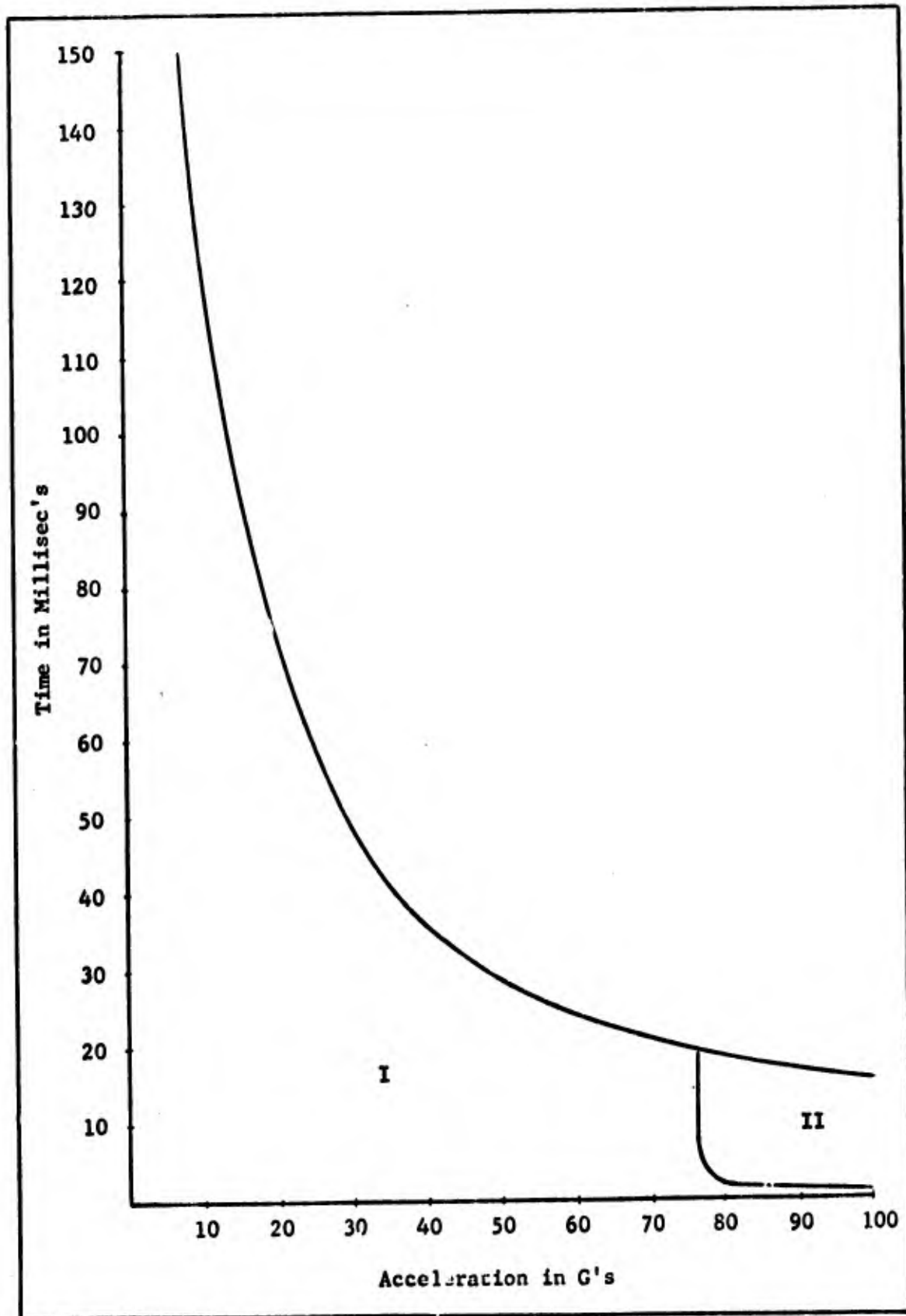


Fig. 22. Time for Maximum Deflection (t_{\max}), $v_2 = 1000$ c.s.
(Low Accelerations)

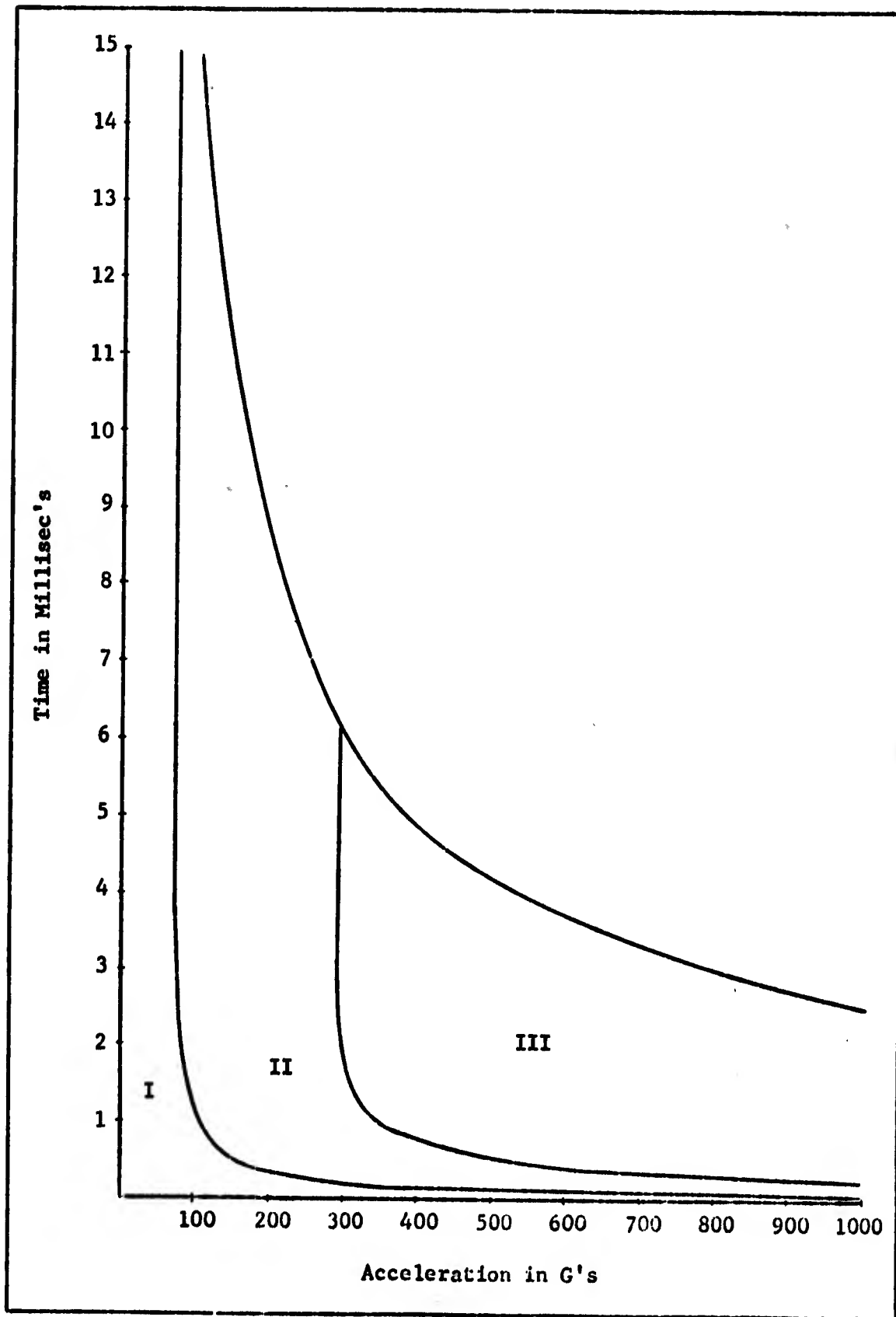


Fig. 23. Time for Maximum Deflection (t_{max}), $v_2 = 1000$ c.s.
(High Accelerations)

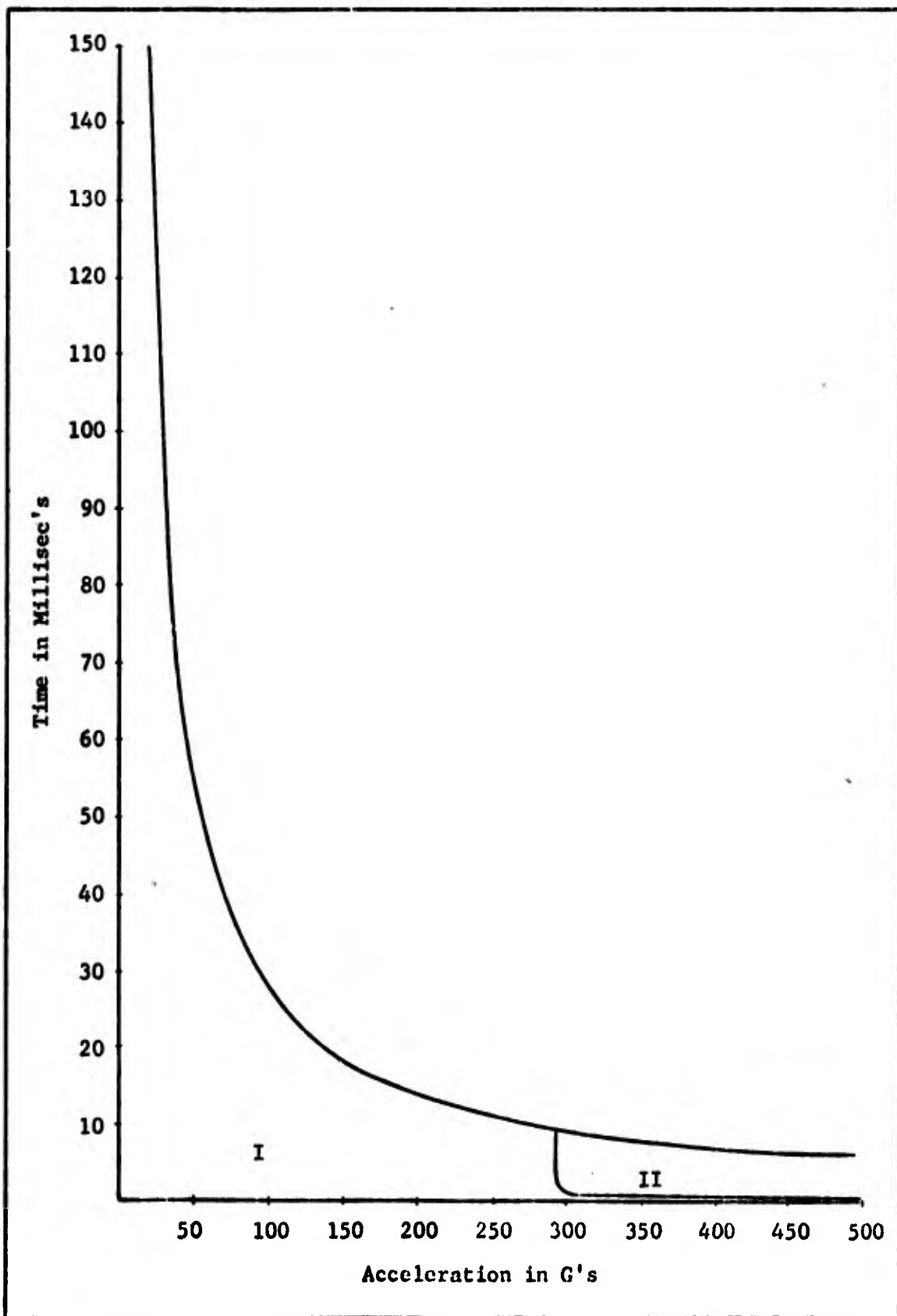


Fig. 24. Time for Maximum Deflection (t_{max}), $v_3 = 2000$ c.s.
 (Low Accelerations)

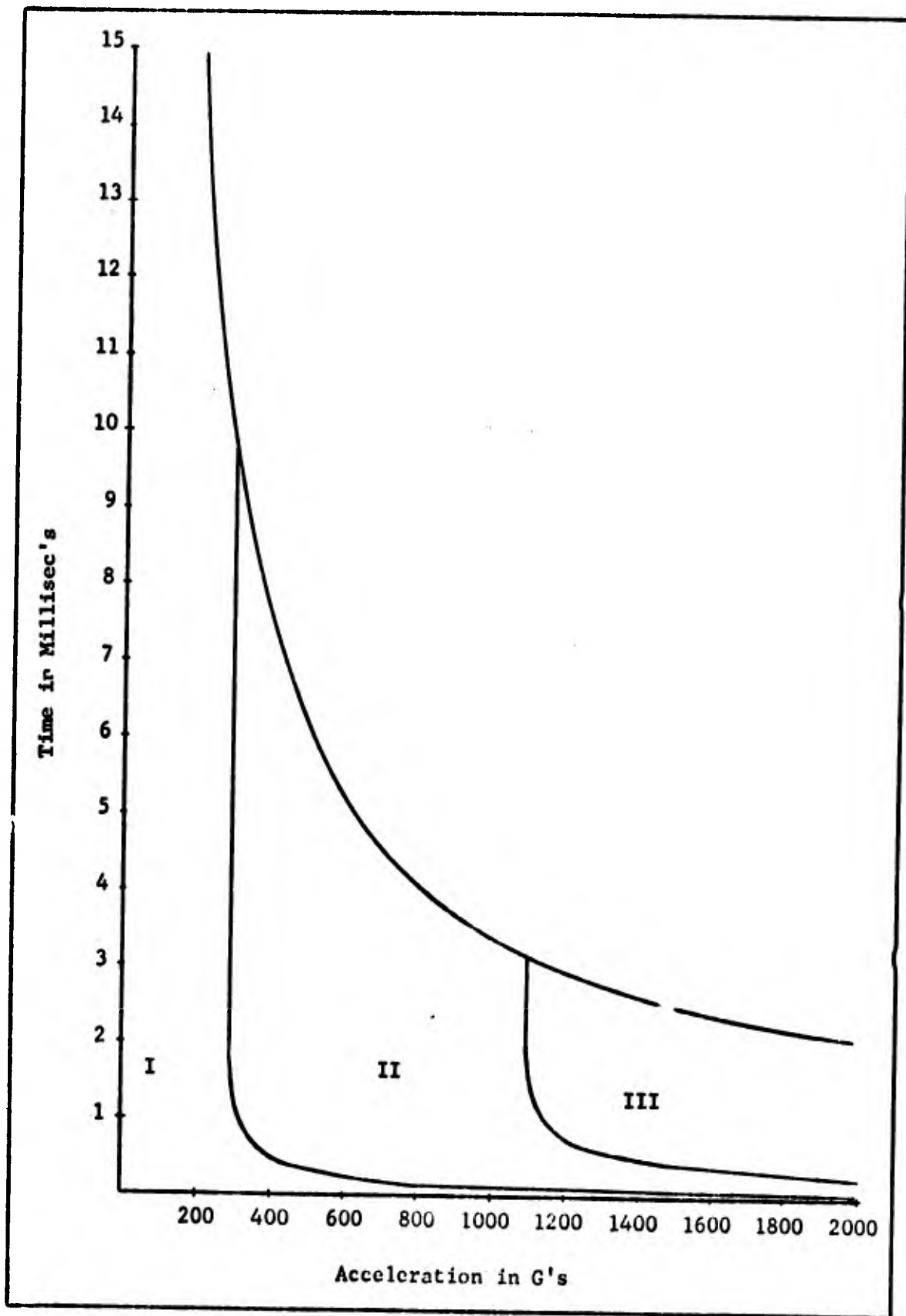


Fig. 25. Time for Maximum Deflection (t_{max}), $v_3 = 2000$ c.s.
(High Accelerations)

Response to a Dynamic Input

Three dynamic inputs were simulated for a gage with 1,000 centi-stoke viscosity oil. This was done to illustrate the dynamic response of the gage in the three operating regions. The input acceleration wave form is shown in Fig. 26.

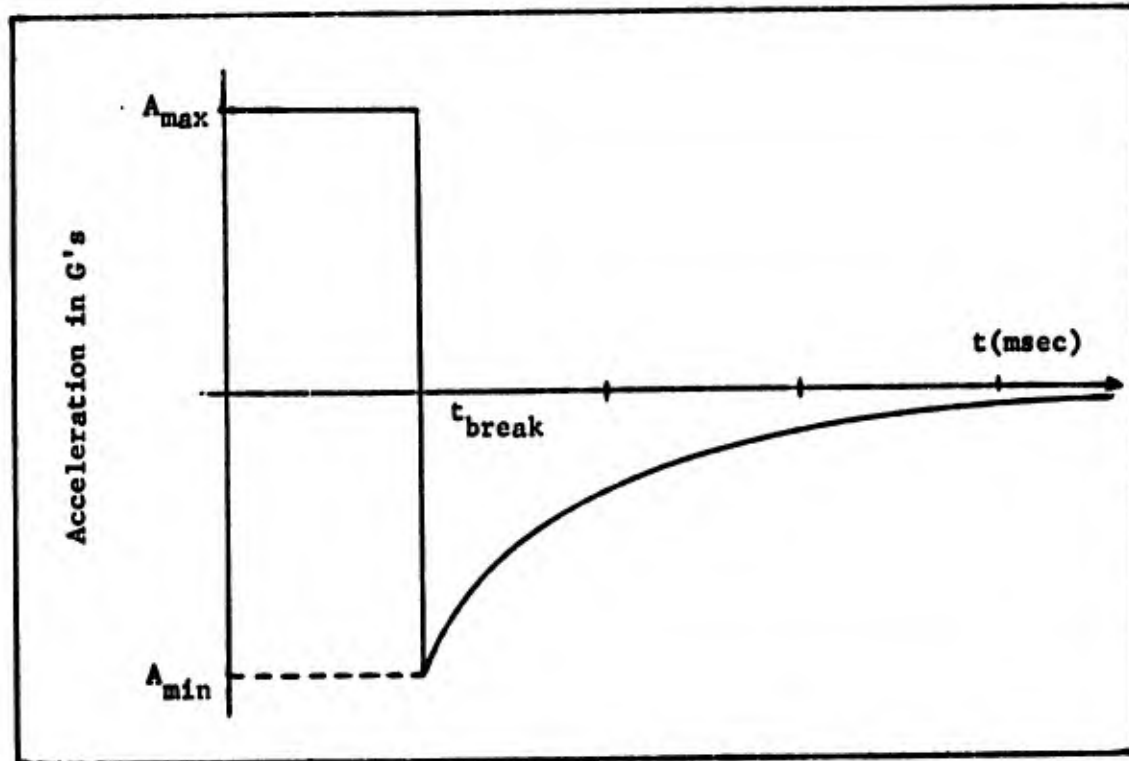


Fig. 26. Input Acceleration Wave Form

The results are shown in Figures 27-29. Each figure shows the normalized velocity and normalized output peak voltage from the simulation.

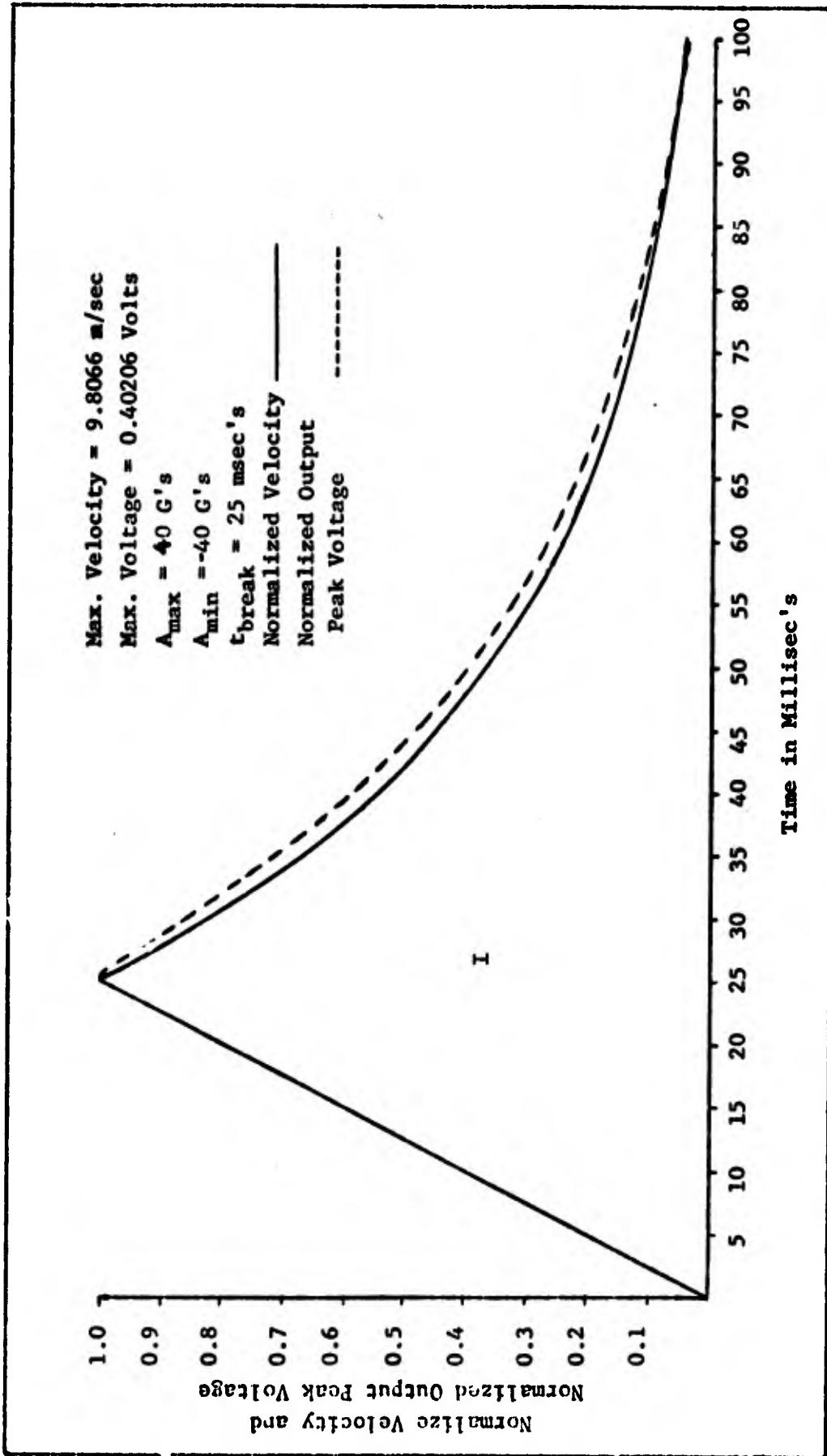


Fig. 27. Comparison of Normalized Velocity and Normalized Output Peak Voltage for 40 G's Peak Acceleration

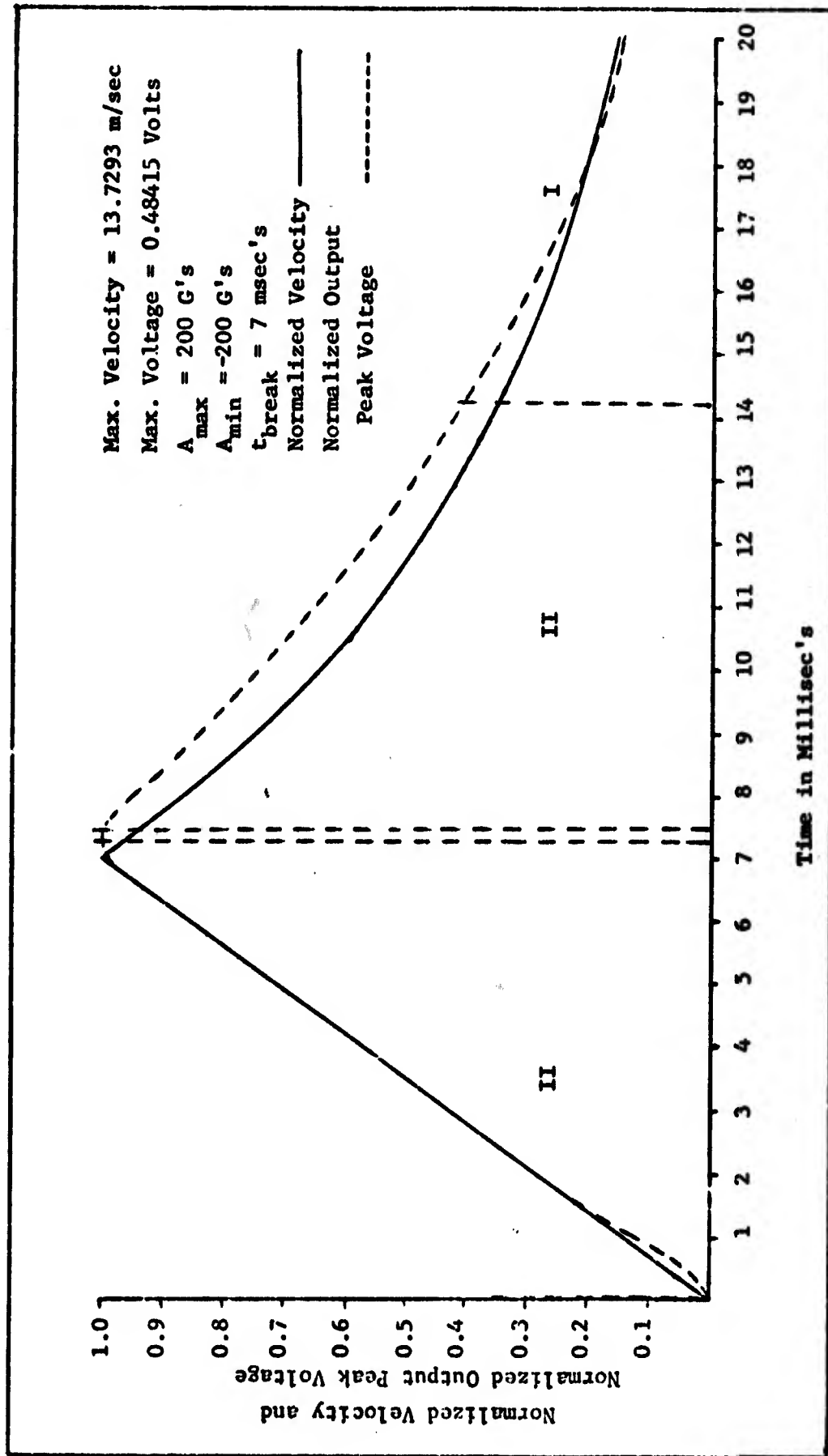


Fig. 28. Comparison of Normalized Velocity and Normalized Output Peak Voltage for 200 G's Peak Accelerations

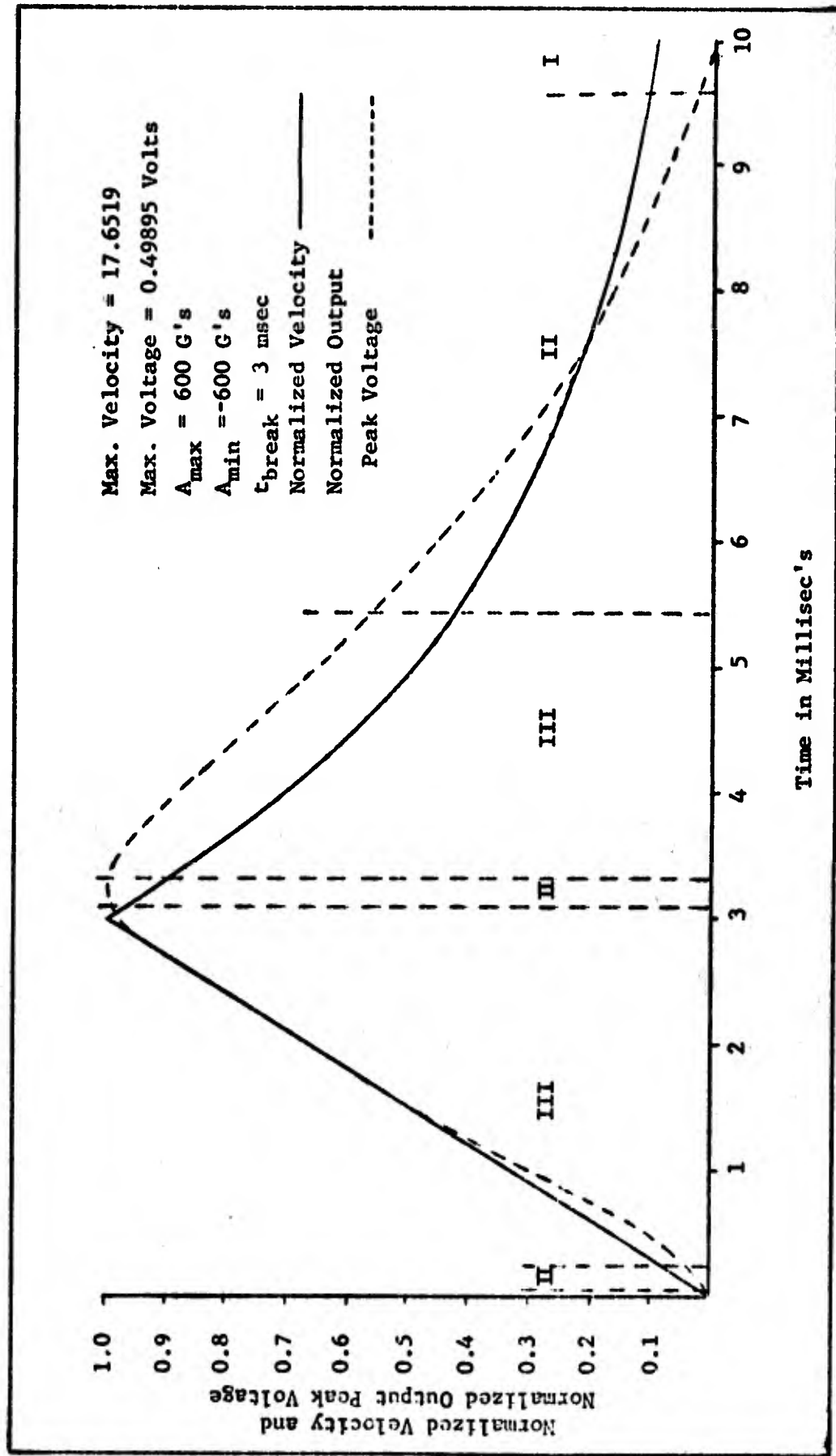


Fig. 29. Comparison of Normalized Velocity and Normalized Output Peak Voltage for 600 G's Peak Acceleration

IV. Conclusions and Recommendations

A state-variable model was developed for the non-linear, time-varying, mechanical-fluidic-electrical system designated as the Sparton 601M Horizontal Velocity Gage. The modeling technique evolved in this research is innovative in that the non-linear, time-varying nature of the damping effect of the oil on the pendulum is included in the model.

The results from the computer simulation of the model have demonstrated:

1. Good correlation between the model simulation and experimental results for the unforced system.
2. The linear and non-linear operating regions of the gage.
3. Acceleration-time limitations for the gage pendulum to remain within the allowable deflection region ($\pm 12^\circ$).
4. Good correlation between the velocity and the peak output voltage for the forced system within the linear operating range of the gage.
5. Degradation of the velocity-output voltage correlation as the operation is forced into the non-linear operating regime.

Additional areas of possible research are recommended as follows:

1. Experimental verification of the model simulation for the forced system with a measurable input and output.
2. Extension of the model to include an acceleration force in an arbitrary direction.
3. Extension of the model to include the data link and demodulation portions of the overall system. (gage-cable-instrumentation van).

Bibliography

1. Swift, L.M. Development of an Earth Velocity Gage. Defense Atomic Support Agency, SRI Project No. SU-2868. Washington, 1960.
2. Perret, W.R., J.W. Wistor, G.J. Hansen, & D.G. Palmer. "Four Papers Concerning Recent Work on Ground Motion Measurements." SC-R-65-905. Sandia Corporation. (July 1965), pp. 25-28.
3. Wong, F.S. "Analysis of Velocity Gage." Agbabian-Jacobsen Associates. Memorandum No. 6726;613 (May 1969).
4. Schultz, Donald G. & James L. Melsa. State Functions and Linear Control Systems. New York: McGraw-Hill Book Company Inc., 1967, pp. 86-87.
5. Synge, J.L. & G.A. Griffith. Principles of Mechanics. New York: McGraw-Hill Book Company, Inc., 1959, p. 177.
6. General Electric Corp. Heat Transfer and Fluid Flow. New York: General Electric Corp., 1970, p. 4.
7. Han, L.S. "Hydrodynamic Entrance Lengths for Incompressible Laminar Flow in Rectangular Ducts." Journal of Applied Mechanics. 27:403-409. (1960).
8. Pai, Shih-I. Viscous Flow Theory. Princeton, New Jersey: D. Van Nostrand Company, Inc., 1956, p. 37.
9. Schlickting, Von H. "Laminare Kanaleinlaufstromung." Zeitschrift fur angewandte Mathematik und Mechanik. 14:368. (1934).
10. Eskinazi, Salamon. Principles of Fluid Mechanics. Boston: Allyn & Bacon, Inc., 1962, p. 14.
11. Dow Corning Corp. Information about Silicone Fluids. (Bulletin 22-0692). Michigan: Dow Corning Corp., 1972.
12. Streeter, Victor L. ed. Handbook of Fluid Dynamics. New York: McGraw-Hill Book Company, Inc., 1961, chap. 1, p. 17.
13. Pender, Harold & Knox McIlwain, ed. Electrical Engineers' Handbook. New York: John Wiley & Sons, Inc., 1950, chap. 2, p. 63.

Appendix A

Computer Program Symbols

Appendix A

Computer Program Symbols

| <u>Computer Symbol</u> | <u>Symbol Used in Model</u> |
|------------------------|-----------------------------|
| A | $\ddot{X}(t)$ |
| AREA 1 | A_{81} and $A_{9 16}$ |
| AREA 2 | A_{67} and $A_{14 15}$ |
| B | β |
| C | c |
| D2 | d_2 |
| D3 | d_3 |
| E | l_{69} and $l_{14 15}$ |
| F(1) | $\dot{x}_1(t)$ |
| F(2) | $\dot{x}_2(t)$ |
| F(3) | $\dot{x}_3(t)$ |
| H1 | $L_1(t)$ |
| H2 | $L_2(t)$ |
| DH1 | $\frac{dL_1(t)}{dt}$ |
| DH2 | $\frac{dL_2(t)}{dt}$ |
| T | t |
| T1 | τ |
| V | $\dot{X}(t)$ |
| V1N | $V_{in}(t)$ |
| VOUT | $V_{out}(t)$ |
| XN | N_1 and N_2 |
| XMU | μ_o |
| X(1) | $x_1(t)$ |

Computer SymbolSymbol Used in Model

X(2)

 $x_2(t)$

X(3)

 $x_3(t)$ Other Computer SymbolsDefinition

DERK

Name of Runge-Kutta subroutine

H

Increment of time

M

Number of state variables

Appendix B

Computer Program Listing

```

PROGRAM MAIN(INPUT,OUTPUT)
DIMENSION X(3),F(3)
PRINT 10
10 FORMAT(1F1,5X,4HTIME,2X,8FVCLCCITY,12X,5FTHETA,5X,
C17DERIVATIVE OF THETA,3X,16FCURRENT IN COILS,3X,
C11FVCLTAGE OUT,3X,10FVCLTAGE IN,5X,7FV/DE FE,7)
XPL = 4.3*3.14159265358979*3000001
XN = 550.0
D2 = 0.00625
D3 = 0.0083853
E = 0.0005
B = 0.17986
AREA1 = 0.000125
AREA2 = 0.00001
15 G = 9.8066352
M = 3
T = 0.0
X(1) = 0.0
X(2) = 0.0
20 A1 = XN**2*AREA1*AREA2*XPL
A2 = SQRT(D3**2+D2**2-2.*D3*D2*CCS(X(1)+E))
A3 = SQRT(D3**2+D2**2-2.*D3*D2*CCS(X(1)-E))
A4 = AREA1*E
H1 = A1/(AREA2*A2+A4)
25 AE = 2.*AREA2**2*D3*D2*SIN(X(1)+E)*X(2)
AF = 2.*AREA2**2*D3*D2*SIN(X(1)-E)*X(2)
DF1 = (-A1*(AE/(2.*AREA2*A2)))/((AREA2*A2+A4)**2)
H2 = A1/(AREA2*A3+A4)
DF2 = (-A1*(AF/(2.*AREA2*A3)))/((AREA2*A3+A4)**2)
30 HL = H1+H2
X(3) = -(14.142135623730)/(2.*3.14159265358979*3000000*HL)
TERM1 = 1./(H1+H2)
TERM2 = DF1+DF2
V = 0.0
35 VIN = 14.142135623730*SIN(2.*3.14159265358979*3000000*T)
VCLT = (-DF1+H1*TERM1+TERM2)*X(3)+(-H1*TERM1+0.5)*VIN
PRINT 7, T,V,(X(J),J=1,M),VCLT,VIN
7 FORMAT(1X,F12.10,7E16.5)
H = 0.0000000000000000
40 INDEX = 1
1 IF(T-0.0070)2,2,5
2 A = 200.0*G
GC TO 4
5 A = -270.0*G*EXP(-142.85714*(T-0.007))
45 4 CONTINUE
IF(T.GT.0.0) GO TO 14
T1 = 1.0
GC TO 15
14 T1 = 2.240/(ABS(X(2)))
50 15 F(1) = X(2)
IF(T1.LT.0.012) GO TO 18
IF(T1.LT.0.06) GO TO 17
IF(T1.LT.0.2) GO TO 16
F(2) = -2458.3*X(2)-358.78*X(1)+36.585*A
55 GC TO 19

```

Reproduced from
best available copy.

```

16 F(2) = -1994.3*X(2)*(ABS(X(2)))**0.0945-358.78*X(1)+36.585*A
GC TC 19
17 F(2) = -1287.4*X(2)*(ABS(X(2)))**0.2173-358.78*X(1)+36.585*A
GC TC 19
50 18 F(2) = -289.67*X(2)*(ABS(X(2)))**0.5003-358.78*X(1)+36.585*A
19 A1 = XN**2*AREA1*AREA2*XPL
A2 = SQRT(C3**2+D2**2-2.*C3*C2*CCS(X(1)+E))
A3 = SQRT(C3**2+D2**2-2.*C3*C2*CCS(X(1)-E))
A4 = AREA1*E
65 H1 = A1/(AREA2*A2+A4)
A5 = 2.*AREA2**2*D3*D2*SIN(X(1)+E)*X(2)
A6 = 2.*AREA2**2*D3*D2*SIN(X(1)-E)*X(2)
CF1 = (-A1*(A5/(2.*AREA2*A2)))/((AREA2*A2+A4)**2)
70 H2 = A1/(AREA2*A3+A4)
DF2 = (-A1*(A6/(2.*AREA2*A3)))/((AREA2*A3+A4)**2)
TERM1 = 1./(H1+H2)
TERM2 = CF1+DF2
VIN = 14.142135623730*SIN(2.*3.1415926535897*3.10*T)
F(3) = -(TERM1*TERM2)*X(3)+TERM1*VIN
75 CALL DERK(M,X,F,T,H,INDEX)
IF (INDEX-1) 3,3,1
3 IF(T-0.0070)11,11,12
11 V = A*T
GC TC 13
80 12 V = 1.4*G*EXP(-142.85714*(T-(.07)))
13 VIN = 14.142135623730*SIN(2.*3.1415926535897*3.10*T)
VCUT = (-CF1+H1*TERM1*TERM2)*X(3)+(-H1*TERM1+0.5)*VIN
PRINT 7, T,V,(X(J),J=1,M),VCL1,VIN,T1
20 IF(T-0.014)1,1,6
85 E STCF
END

```

Reproduced from
best available copy.

```

SUBROUTINE DERK(M,X,F,T,H,INDEX)
DIMENSION X(100),F(100),Q(400)
GO TO (18,19),INDEX
5      18      KXX=0
          INDEX=2
          DO 35 I=1,M
          J=I+300
          35      Q(J)=X(I)
          19      KXX=KXX+1
          10      GO TO (1,2,3,4),KXX
          1      DO 5 I=1,M
          Q(I)=F(I)*H
          5      X(I)=X(I)+Q(I)/2.
          T=T+H/2.
          15      RETURN
          2      DO 5 I=1,M
          J=I+100
          K=I+300
          Q(J)=F(I)*H
          20      6      X(I)=Q(K)+Q(J)/2.
          RETURN
          3      DO 7 I=1,M
          J=I+200
          K=I+300
          25      Q(J)=F(I)*H
          7      X(I)=Q(K)+Q(J)
          T=T+H/2.
          RETURN
          4      DO 8 I=1,M
          J=I+100
          K=I+200
          L=I+300
          30      8      X(I)=Q(L)+((Q(I)+2.*Q(J)+2.*Q(K)+F(I)*H)/5.)
          INDEX=1
          35      RETURN
          END

```